

Normal and Abnormal Early Pregnancy

¹Ulrich Honemeyer, ²Asim Kurjak, ³Giovanni Monni

¹Specialist in Obstetrics and Gynecology, Department of Mother and Child, Welcare Hospital, United Arab Emirates, Dubai

²Professor, Department of Obstetrics and Gynecology, Medical School University of Zagreb, Croatia

³Professor, Department of Obstetrics and Gynecology, Prenatal and Preimplantation Genetic Diagnosis, Fetal Therapy Ospedale Microcitmico, Cagliari, Italy

Correspondence: Ulrich Honemeyer, Specialist in Obstetrics and Gynecology, Department of Mother and Child, Welcare Hospital United Arab Emirates, Dubai, e-mail: ulrich@welcarehospital.com

ABSTRACT

The first trimester, mostly defined as the first 100 days of pregnancy, is characterized by many important landmarks heralding the ultimate outcome of pregnancy. Woman becomes aware of her pregnancy after missing her period, being already two weeks postconception at that time. A positive pregnancy test opens Pandora's Box, raising more questions than giving answers. Although a positive pregnancy test most likely suggests an intrauterine pregnancy, production of human chorionic gonadotropin (hCG) occurs as well in tumors (dysgerminoma, choriocarcinoma) or maldeveloped pregnancies, such as ectopic pregnancy, blighted ovum or mola hydatidosa. Other early pregnancy complications and failures, like subchorionic hematoma, missed abortion, incomplete miscarriage, retained products of conception, are likely to be accompanied by clinical symptoms such as lower abdominal pain and/or vaginal bleeding, and suboptimal beta hCG serum levels. Transvaginal ultrasound probes with frequencies of up to 14 MHz have lowered the threshold for US-detection of intrauterine pregnancy to 1200 mIU/ml beta hCG/serum (discriminatory zone), and enable identification of all above-mentioned 1st trimester pregnancy disorders earlier than ever before. Furthermore, the additional interrogation of the region of interest (ROI) with color Doppler (CD) and pulsed-wave Doppler (PW) supplies important information about characteristics of vascularization and flow indices, which assists in further differentiation and prognosis of abnormal early pregnancy findings. With the introduction of transvaginal three-dimensional (3D) sonography, and real-time 3D ultrasound (4D), *in vivo* studies of the early fetal life became possible. The developmental progress of the embryo and early fetus, its anatomy, and first movement patterns, have been explored by means of ultrasonic 3- and 4D imaging, which can be considered as nonteratogenic as long as investigators adhere to certain safety rules. The new field of sonoembryology has emerged, and researchers are penetrating the mists hiding the beginning of human life. Another area of remarkable expansion has been the 1st trimester scan between 11 and 13/6 weeks of gestation. It includes not only the early diagnose of fetal structural anomalies, like acranium-anencephalus sequence, and the screening for fetal aneuploidies such as trisomia 21, 18 and 13, but also offers likelihood ratios for hypertensive pregnancy disorders (pre-eclampsia) and intrauterine growth restriction (IUGR).

Keywords: Sonoembryology, Early pregnancy failure, 3- and 4D ultrasound in early pregnancy, First trimester screening, Structural fetal anomalies, Yolk sac, Preeclampsia.

INTRODUCTION

Ultrasonographic evaluation of pregnancy during the first trimester has no longer the limited purpose of confirmation of viability and gestational age. The amazing improvement of technical equipment and deepened knowledge of embryonic and early fetal development have brought sonomorphologic exploration of pregnancy forward into 1st trimester and changed the agenda of ultrasound examinations in this pregnancy section. Sonographic assessment during 1st trimester targets now ovulation, conception, embryo and early fetus. It is obvious that diagnosis of abnormal early pregnancy, pregnancy failure, and fetal abnormalities should be ascertained as early as possible to enable timely decisions about management. However, newly gained insights have also pointed out the limitations of early ultrasound diagnosis. The sono-anatomic survey of the fetus after 11 weeks' gestation is more likely to produce usable information than before, simply because physiologic structural alterations of the embryo, such as herniation of bowel into the proximal umbilical cord, have disappeared. Moreover, advanced ossification after 11 weeks permits assessment of cranial vault and nasal bone. The introduction of 3D, real-time

3D (4D), color and power Doppler and their attachment to transvaginal scanning has boosted our knowledge of early pregnancy ever more. Reports of new findings arrive almost monthly. All this should not let sonographers forget about safety of ultrasound in embryonic and early fetal diagnosis.

Acute Pelvic Pain in the First Trimester

Ectopic pregnancy, and other causes like threatened abortion, inevitable abortion, failed intrauterine pregnancy, subchorionic hematoma, spontaneous abortion, 1st trimester pregnancy failure and vaginal bleeding can be reason for pelvic pain.¹

Clinical signs, such as abdominal pain and vaginal bleeding in early pregnancy, are in first line suspicious of spontaneous abortion. Ultrasound supports the differentiation into threatened, incomplete or complete abortion and shows the way to appropriate clinical management. About 30 to 40% of pregnancies fail after implantation, but only 10 to 15% manifest with clinical symptoms.²

However, vaginal bleeding in first trimester may as well be symptom for a variety of other early-pregnancy pathologies, such as missed abortion, blighted ovum and ectopic pregnancy.

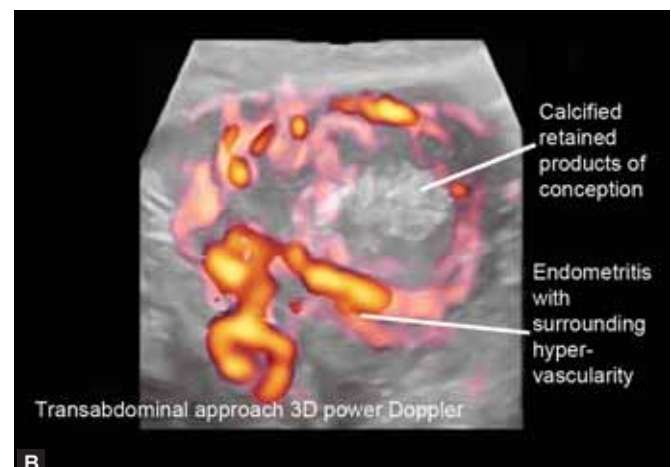
Vaginal bleeding and incomplete and complete spontaneous abortion, retained products of conception (RPoC) are the causes of bleeding and often endomyometritis, even septic complications. Transvaginal ultrasound with color Doppler is the key to a correct diagnosis in these cases. Intrauterine masses with heterogeneous echoes, with or without vascularization in color Doppler, together with anamnestic information of secondary amenorrhea and/or positive beta hCG testing, are suggestive of RPoC and require dilatation and evacuation (D&E) (Figs 1A and B).

An empty uterine cavity, however, with reliable proofs for a previous intrauterine GS and positive beta hCG test, represents findings of a complete miscarriage and absolve the clinician from the necessity of D&E of RPoC. Catastrophic developments can be caused by wrong diagnosis of cervical ectopic pregnancy as 'cervical abortion', when D&E brings about the risk of profuse bleeding that may need radical approaches, such as emergency hysterectomy. Such deleterious diagnostic misunderstandings can only be avoided by thorough anamnestic and clinical evaluation, and the use of transvaginal color Doppler US for detection of atypically increased vascular signals around the suspected RPoC in the cervix (Figs 2A and B).

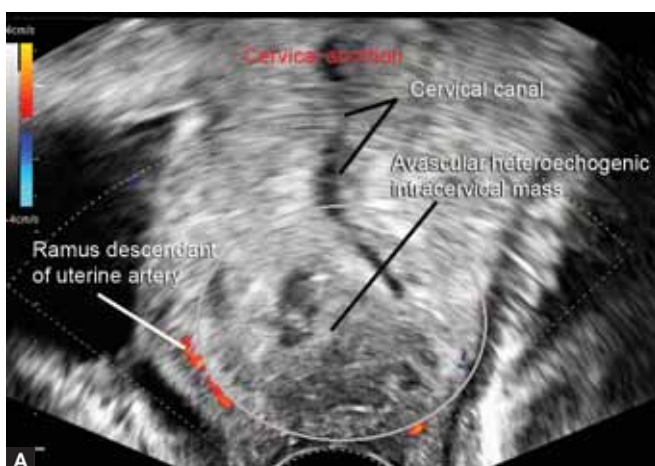
Missed abortion: The diagnose of missed abortion is determined by sonographic demonstration of an embryo or fetus without cardiac activity. Since cardiac activity is first seen at 6 weeks, the diagnosis of missed abortion requires repeated TVS with color Doppler, and serum beta hCG time profile over at least 48 hours, in cases, where embryo CRL measurements equal 6 weeks or less of gestational age (GA) (Figs 3A to E).

Blighted ovum: The term refers to a GS in which the embryo either failed to develop or died at a stage too early to visualize with 14 MHz high resolution TVS probe. Blighted ovum can be diagnosed at a mean GS diameter of 15 mm. If the volume of the GS is less than 2.5 ml and is not increasing in size by at least 75% over a period of one week, the requirements for diagnosis of blighted ovum are fulfilled. This may further be supported by serial nonascending serum beta hCG levels during this week (Figs 4A to C).

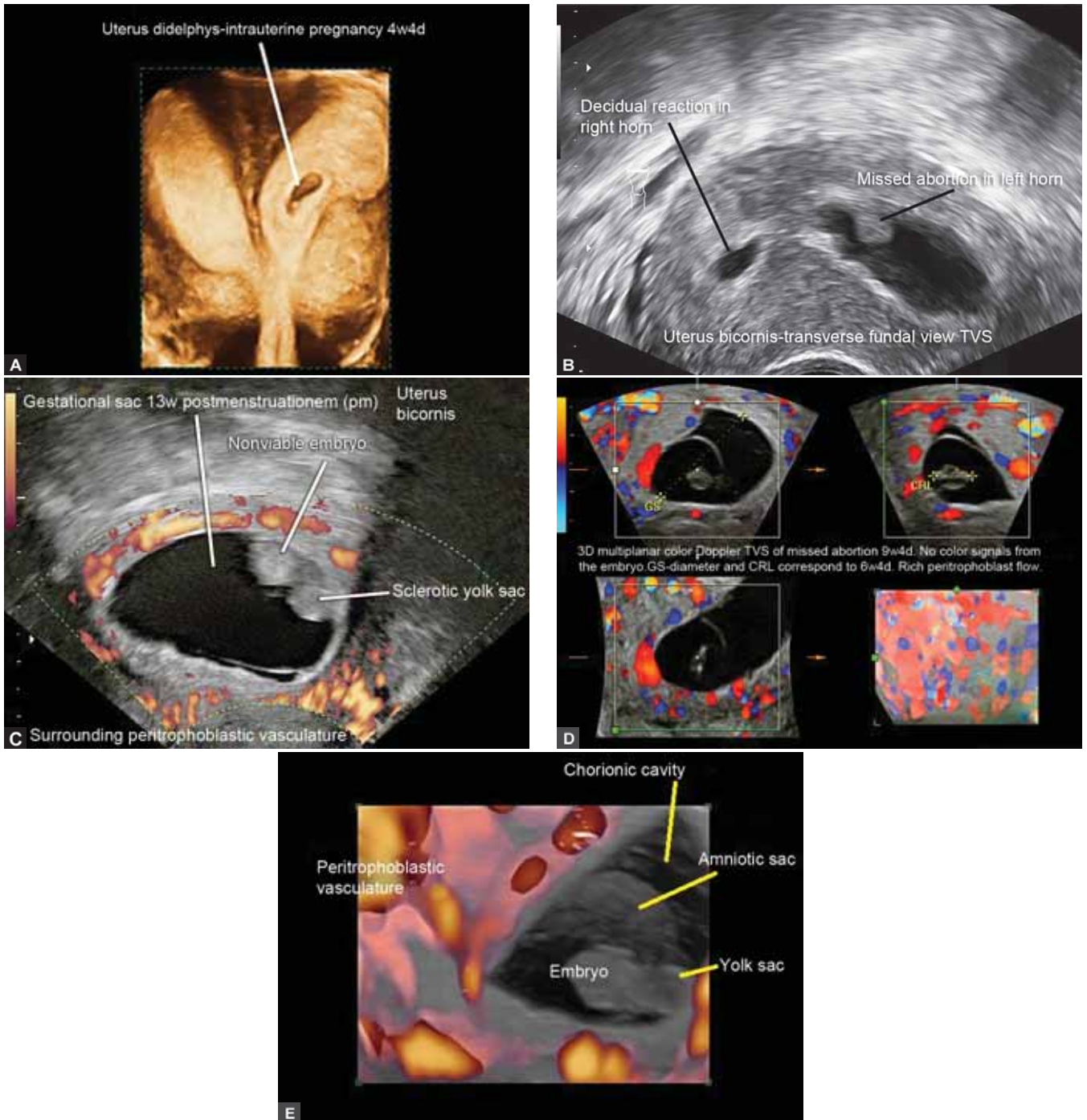
Intrauterine hematoma in early pregnancy: Intrauterine hematomas can be, according to their location, divided into retroplacental, subchorionic, in fundal or cervical. Cervical hematomas are likely to find drainage through the cervical channel; the threat of pregnancy loss for the patient is



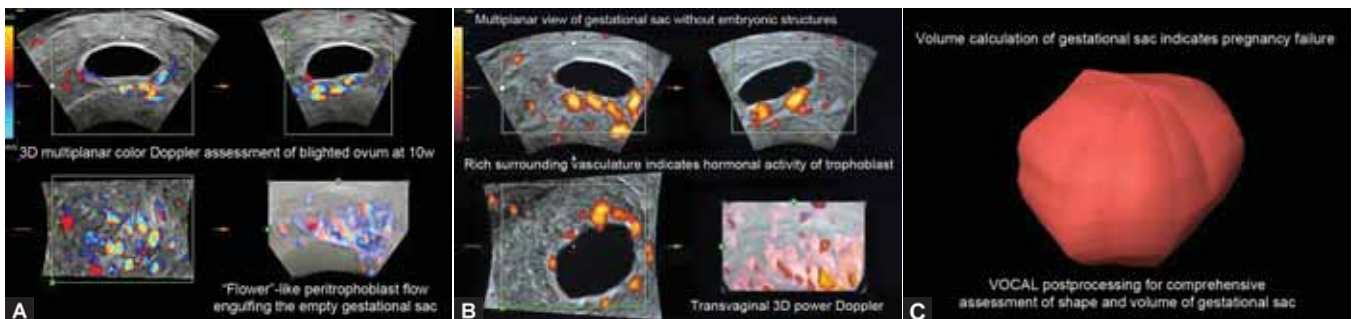
Figs 1A and B: Retained products of conception in B-mode and 3D power Doppler



Figs 2A and B: Cervical abortion and cervical pregnancy



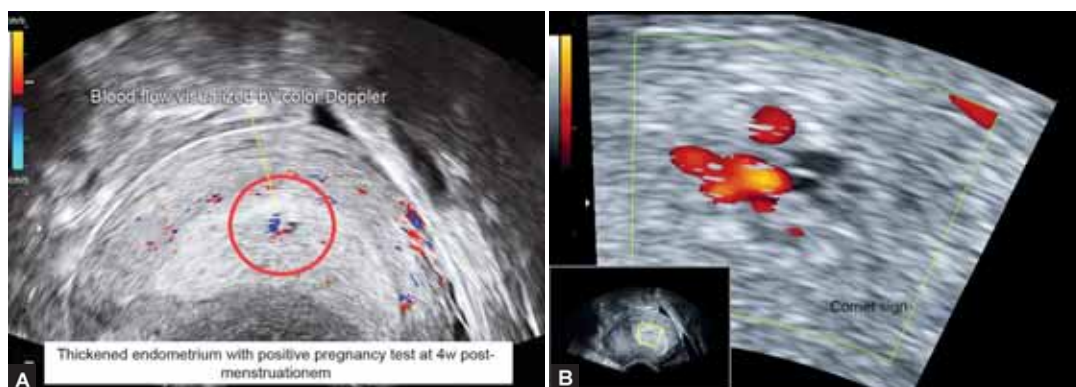
Figs 3A to E: Pregnancy in uterus didelphys, missed abortion in uterus bicornis, missed abortion multiplanar and in 3D power Doppler mode



Figs 4A to C: Blighted ovum in multiplanar color Doppler, multiplanar power Doppler with VOCAL



Figs 5A to C: Subchorionic hemorrhage in B-mode, 3D surface rendered and 3D color Doppler



Figs 6A and B: Comet sign color and power Doppler

emphasized by vaginal bleeding. The prognosis, however, is much better in a cervical than in a fundal hematoma, because in the fundal hematoma, without chance of decompression, uteroplacental circulation via spiral arteries is soon compromised. Kurjak et al reported an increased resistance to blood flow and reduced velocities in spiral arteries on the side of the hematoma, as a result of mechanical compression caused by the hematoma.³

It is likely that if the bleeding occurs below the area of cord insertion, at the level of the definitive placenta, this incident may finally result in separation of the placenta and abortion. Vice versa, a hemorrhage opposite of the umbilical cord insertion could probably reach a much higher volume before causing detachment of the placenta from the main area of spiral artery blood supply (Figs 5A to C).

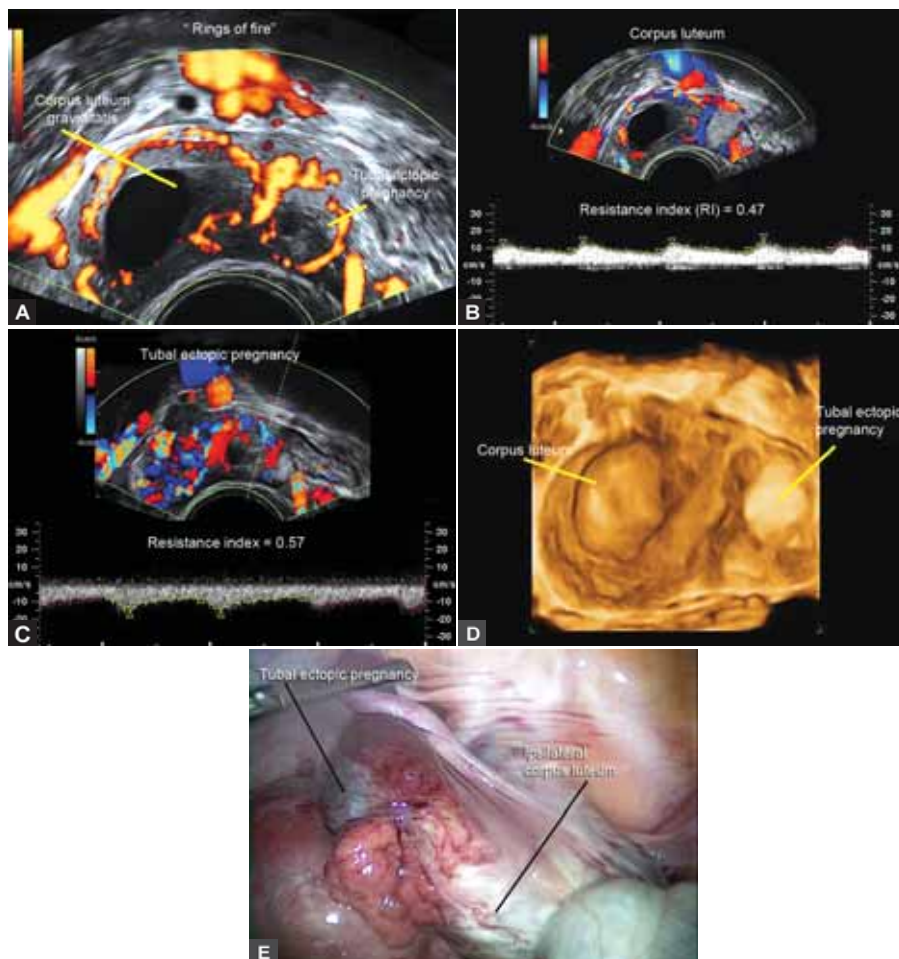
Ectopic pregnancy: It is a common cause of acute abdomen in emergency units, with an incidence of 20 per 1000 pregnancies. Ectopic pregnancy constitutes the leading cause of pregnancy-related maternal deaths in the 1st trimester and accounts for 4 to 10% of all pregnancy-related deaths. About 6 to 10% of all pregnant women who go to an emergency department with 1st trimester bleeding, pain, or both, have an ectopic pregnancy.⁴⁻⁶

The most common extrauterine pregnancy location is the fallopian tube, which accounts for 98% of all ectopic gestations. The major cause of tubal pregnancy is disruption of normal tubal anatomy, as consequence of pelvic inflammatory disease (PID), surgery, congenital anomalies, or tumors, causing anatomic distortion, damaged ciliary activity, and thus impaired function of the fallopian tube. High-risk factors for ectopic

pregnancy include previous ectopic pregnancy, tubal surgery, exposition to DES (diethylstilbestrol) *in utero*, and intrauterine contraception with a copper intrauterine device (IUD).⁷

Discriminatory zone: At a serum beta hCG level of 1500 mIU/ml, which is reached at day 10 to 14 pc in a normal gravidity, an intrauterine chorionic sac can be detected by TVS probe with minimum 5 MHz frequency. In transabdominal US, serum beta hCG values may have to be as high as 6500 mIU/ml before an intrauterine gestational sac is detected. These serum beta hCG levels mark the so-called discriminatory zone in which discrimination of a normal intrauterine chorionic sac should be possible. In a normal intrauterine pregnancy, a chorionic sac is visible at 4.5 to 5 weeks' gestation presenting a double echogenic ring around a hypoechoic GS, with eccentric embedding in the decidua. The 'Comet sign' of intervillous flow in PD assessment of the decidua around the double echogenic ring, and visualization of a yolk sac at 5w+, confirm the impression of an intrauterine implantation (Figs 6A and B).

Conversely, in patients with beta hCG of 1500 mIU/ml and more, an empty uterine cavity visualized by TVS with specifications as above can be taken as indirect proof for ectopic pregnancy. An ectopic pregnancy can occur as pregnancy with viable embryo in 10%, as blighted ovum in 40%, and as questionable adnexa in 50% of cases. Color and power Doppler demonstrate randomly dispersed multiple small vessels within the adnexa, with pulsed-wave (PW) Doppler showing resistance-to-flow as low as RI < 0.42. Color-coded flow signals of the ectopic pregnancy are clearly separated from ovarian tissue and



Figs 7A to E: Ectopic pregnancy, neighboring corpus luteum, assessment of flow velocities, color-power Doppler imaging of 'ring of fire', laparoscopic aspect

corpus luteum. The extent of vascularity reflects trophoblastic vitality and invasiveness (neoangiogenesis), enhanced by vasodilatation of the fallopian vessels under the influence of maternal progesterone.⁸

Visualization of the characteristic corpus luteum blood flow may aid in diagnosis of ectopic pregnancy, since about 85% of all ectopic pregnancies are found on the very same side of the corpus luteum. This explains why in the majority of cases with proven ectopic pregnancy, luteal flow is detected ipsilateral of the ectopic pregnancy. Luteal color or power Doppler flow may be used as a guide while searching for an ectopic pregnancy and could be called the 'light house-effect' of corpus luteum, which directs the investigator to the color Doppler signals of the ectopic pregnancy (Figs 7A to E).^{9,10}

Sonographic and clinical assessment, taking into account sonographic parameters such as size of the ectopic, if visualized, vascularity, indirect signs of instability like hemoperitoneum, together with information about duration of secondary amenorrhea and biochemical data of serum beta hCG levels, will lead to correct diagnosis and help in deciding about conservative or surgical management options.

Screening for fetal malformations: Although the 1st trimester screening could not completely replace the standard

mid-trimester scan for structural anomalies, different studies have shown that it is possible to identify fetal abnormalities and detect genetic syndromes already in the 1st trimester scan.^{11,12}

It is not unusual for obstetricians and gynecologists to have ultrasound equipment in their private offices. Radiologists usually have either a hospital-based practice or function in a free-standing diagnostic imaging center. For using diagnostic ultrasound, the gynecologist/obstetrician clinician must have solid basis and detailed knowledge about gynecological/fetal cross sectional anatomy. Also important for the clinician is, to know her or his limits in regards to ultrasound diagnosis. However, basic and limited scans in an Obstetrician/Gynecologist office can provide useful first-stage diagnostic information, and a fetus with suspected structural anomalies should then be referred to a tertiary center where confirmation of the suspicion and search for associated anomalies can follow. In this context, it is interesting to know that only 35% of all 1st trimester studies carried out in obstetric practice have been found to meet all ACOG criteria¹³ and only 15% to meet all AIUM criteria for documentation. First trimester reports from radiologists met ACOG criteria only in 11.5% and AIUM criteria only in 4% of the cases.¹⁴

There is proof as well that ultrasound scan is not effective in detecting fetal malformation if used at a basic level.¹⁵

If the primary indication for obstetric sonography is to diagnose or exclude congenital anomalies (targeted sonography), then this study should be performed in a center where special expertise is available and has been demonstrated.¹⁶

Safety of Ultrasound in Embryonic and Early Fetal Diagnosis

Sonographers are responsible for safety of ultrasound and should be aware that intense ultrasound could damage embryonic tissue. Teratogenicity has been reported in animal fetuses exposed to high temperature. Since the main biological effect of ultrasound absorption in tissue is an increase of temperature (thermal effect), users of diagnostic ultrasound should be familiar with the ultrasonic intensity of their machines and with methods to prevent thermal hazards to the embryo. On the screen of all modern machines, the thermal index (TI) of any scanning activity is continuously displayed. TI 1 stands for 1°C temperature elevation above 37°C and, for example, TI 3 means a temperature rise of 3° from 37 to 40°C in the tissue. The difference between ultrasonic physiotherapy and diagnostic Doppler ultrasound is only the duration of exposure, whereas both operate with maximum intensities of 1 to 3 W/cm². Temperature increases not only in the sample volume, but also in all tissue layers passed on the way. Thermal effect is, therefore, a big concern in diagnostic Doppler ultrasound. It is more pronounced in pulsed-Doppler (PW) than in color/power Doppler flow mapping. Hence, great care has to be taken in scanning febrile patients where the basic temperature is higher than 37°C, regarding exposure time.¹⁷

Ethics of First Trimester Screening

The obstetrician as fiduciary of the pregnant patient has the obligation to provide all necessary information for the patient to enable her autonomy in the management of her pregnancy. The 1st trimester combined screening for trisomy 21 has been shown to be a reliable screening tool that should be introduced to all pregnant women as soon as they are diagnosed to be pregnant in the 1st trimester. Communicating the result of the risk assessment to the patient enhances her autonomy by allowing her an informed decision about options of diagnostic tests, like chorionic villus sampling (CVS) or amniocentesis and, depending on the diagnosis, the continuation of the pregnancy. Recent data demonstrate that women in Australia, Europe and the United States want this information. The risk assessment should be offered in a high quality center, and the option of risk assessment should be presented nondirective. The same applies to counseling of the patient after obtaining an 'elevated risk' result of the 1st trimester screening in regards to the next invasive steps (CVS, amniocentesis), and especially after receiving the results of the invasive tests.¹⁸

First Trimester Combined Ultrasound Screening

There is more to 1st trimester ultrasound than to establish viability of the fetus and accurate gestational age. The utility of the 11 to 13+6 weeks scan continues to expand, presently including evaluation of the fetus morphology, of the maternal pelvic vasculature, and the maternal serum. The aim is to give precise risk estimates of fetal aneuploidy and reliable forecasts on incidence of intrauterine growth restriction (IUGR) and pre-eclampsia. The screenings focus is the most common fetal aneuploidy trisomy 21; however, it assists as well in detection of other chromosomal disorders, such as trisomy 18 and 13, monosomy X, triploidies and aneuploidies involving the sex-chromosome.¹⁹

Two main advantages of the 1st trimester screening for aneuploidies and structural anomalies have been acknowledged: First, early reassurance of fetal well-being reduces both maternal anxiety and uncertainty regarding the present gestation. Second, early diagnosis of an abnormal fetus allows decision making and potentially subsequent termination of pregnancy (ToP) in the 1st trimester when complication rates are lower.²⁰ First trimester ultrasound screening should include maternal age, NT as ultrasound marker and PAPP-A, and free β -hCG as biochemical markers. These parameters have a detection rate of 90.0% at 5.5% false-positive rate for trisomy 21, detection rate of 75.0% at 1.0% false-positive rate for trisomy 18 and detection rate of 87.5% at 5.2% false-positive rate for all aneuploidies. In normal fetuses, the ductus venosus (DV) waveform shows a peak velocity during ventricular systole, another peak during ventricular diastole and a nadir during atrial contraction. In combination with NT, DV and biochemical markers, the absence of the nasal bone indicates the possibility of a chromosomal anomaly. By introducing the nasal bone as an independent additional ultrasonographic marker, and by using color Doppler evaluation of DV as a second line marker, the detection rate of trisomy 21 can be increased to 98%, at 5% false-positive rate. Results of different studies suggest that NT should be used as a first-line screening test in order to maintain the sensitivity, while examination of the DV waveforms can be useful as a second-line test in order to decrease the false-positive rate, reducing the need for invasive testing to less than 1%.²⁰

To understand the significance of each ultrasound marker, it is helpful to contemplate that these markers are foreboding the postnatal phenotype first described by Langdon Down in 1866. Skin that appears too large for their body (increased nuchal translucency), small nose (hypoplastic or absent nasal bone), flat face (frontomaxillary facial angle, FMF > 90°). Even the recently added markers tricuspid regurgitation and reversed A-wave of ductus venosus find perspicuous explanation in early manifestations of abnormal microscopic and ultrastructural anatomy of the fetal myocardium and valve leaflets. These changes result in dilatation of the tricuspid valve annulus with systolic regurgitation of blood from the right ventricle back



Fig. 8A: Ideal fetal midline section of head and upper thorax



Fig. 8E: Tricuspid valve regurgitation demonstrated by power Doppler



Fig. 8B: Increased nuchal translucency

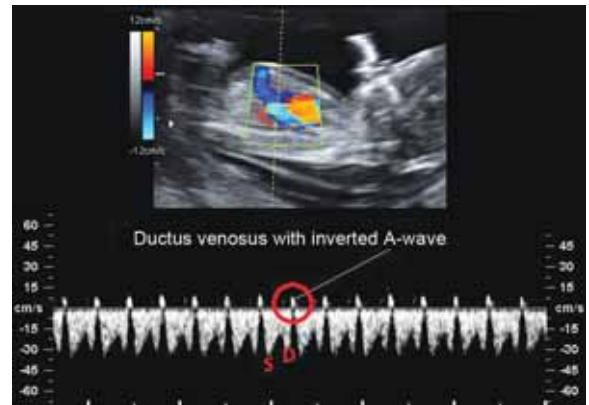


Fig. 8F: Reversed ductus venosus A-wave



Fig. 8C: Absent nasal bone



Fig. 8G: Increased NT with tricuspid regurge and reversed A-wave at 12w3d, entire fetus 3D surface view

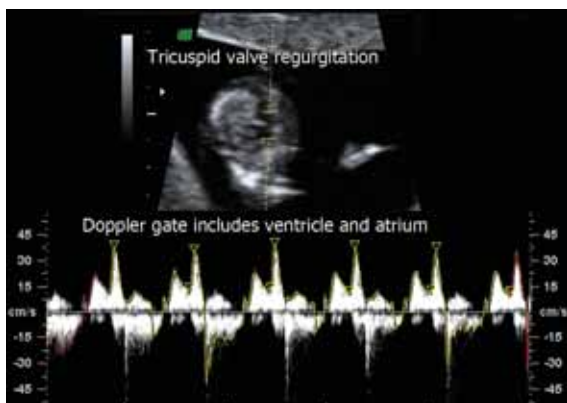


Fig. 8D: Tricuspid valve regurgitation

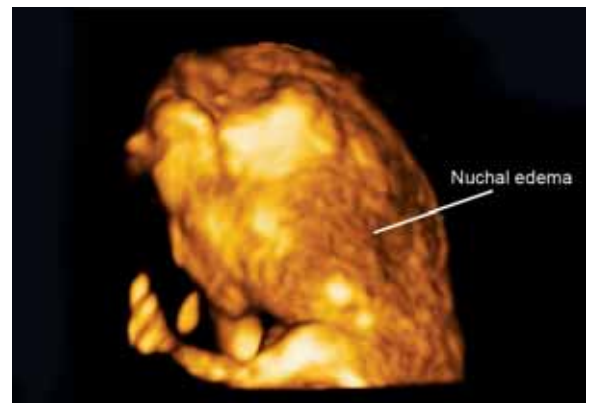


Fig. 8H: Increased NT at 12w3d, head and shoulders, 3D rendered surface view

into the right atrium, and transmission of this regurge into the ductus venosus (positive A-wave) (Figs 8A to H).²¹

What is New in 1st Trimester Screening?

Intracerebral translucency: Other than the exencephaly-anencephaly sequence, open neural tube defects (NTD) were always difficult to diagnose at 1st trimester screening. This deficiency is probably rectified by introduction of the new marker intracerebral translucency (IT).²²

The fetal image which is needed to evaluate IT, is the same as for NT, FMF angle and nasal bone assessment: A magnified midline view of the fetal head and upper thorax with depiction of the hypoechoic regions of the thalamus, the pons (brain stem) and the medulla oblongata. The morphological equivalent of the IT is the fluid-filled fourth ventricle posteriorly of the pons. Posterior border of the pons and floor of fourth ventricle compose a thin echogenic line delineating the anterior circumference of the IT, whereas the roof of the fourth ventricle represents the posterior border of the IT (Fig. 9).

A total of 200 fetuses subsequently confirmed not to have NTD showed normal IT appearance at 1st trimester screening. Four fetuses however, during 2nd trimester screening diagnosed to have spina bifida, had absence of IT in the 1st trimester screening (Chaoui et al 2009). The proposed mechanism for this finding is similar to that of the Chiari type II-malformation with 'banana sign', visible in 2nd trimester fetuses with spina bifida aperta. In Chiari type II-malformation, the open spina bifida leads to a decreased pressure in the subarachnoid spaces with consecutive caudal displacement of the brain, causing obliteration of the fourth ventricle. On the basis of these findings, absence of IT during the 1st trimester screening should trigger an intensive search for NTD, with follow-up at 16 and at 20 weeks.²²

First trimester screening for pre-eclampsia: More than 60 years ago, Ernest Page formalized the concept that placental perfusion was reduced in gestosis.²³



Fig. 9: Magnified fetal midline profile with NT and intracerebral translucency^{27,28}

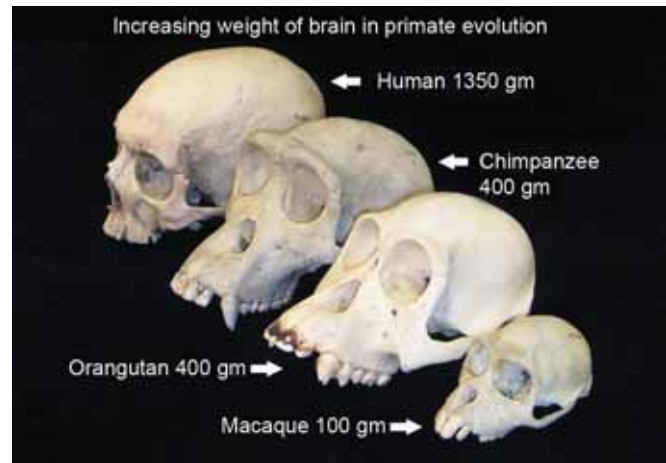


Fig. 10: Increased size of the human brain compared to other primates

Hypertensive disorders of the pregnancy affect approximately 10% of pregnancies. One of the primary causes appears to be a defect of the normal human-specific deep endovascular invasion of the trophoblast, brought by evolution as a consequence of nutritional demands of the increased size of the human fetal brain. The occurrence of pre-eclampsia (gestosis) represents a reproductive disadvantage unique to humans compared with other mammals and primates with a more shallow trophoblast invasion (Fig. 10).^{24,25}

The main threat in pregnancies complicated by gestosis originates from prematurity, intrauterine growth restriction (IUGR) and maternal eclampsia or HELLP syndrome. A two-stage model of gestosis has been proposed to explain its pathophysiology:

- 1st stage of abnormal implantation/trophoblast invasion/vascular remodeling causing reduced placental perfusion and
- 2nd stage leading to the multisystemic maternal syndrome of pre-eclampsia (gestosis).²⁶

The questions: (A) 'why does reduced placental perfusion lead to gestosis?' and (B) 'what exactly links stage 1 with stage 2?', still remain widely unanswered.

Stage 1: Reduced placental perfusion is according to manifold scientific evidence, a result of failed endovascular trophoblast invasion, which is normally processed in an early wave around 10 to 12 weeks, and a second wave being completed around 20 weeks. In normal pregnancies, the embryonal cytotrophoblast cells invade maternal decidua and myometrium, finding their way into the endothelium and highly muscular tunica media of the maternal spiral arteries. As a result of this invasion, the maternal uterine spiral arteries are transformed from muscular arteries with elastic lamina into flaccid tubes, with a vascular radius four times wider than before, turning the placental vascular bed into a low resistance-to-flow area for both fetal and maternal arterial inflow. In gestosis, however, cytotrophoblast cells infiltrate the decidua but fail to penetrate the maternal myometrium.^{27,28}

The successful invasion and transformation appears to depend on a functioning interaction between maternal decidua and fetal trophoblast. Until 10 to 12 weeks, the intervillous space is a low-oxygen environment. With increasing perfusion by maternal spiral arteries, the oxygen tension increases. Local oxygen tension and maternal antioxidant capacity seem to play a critical role in this interaction between decidua and trophoblast, which—if failing—may result in impaired invasion, poor placental perfusion and eventually systemic maternal endothelial dysfunction, the complete picture of gestosis.²⁹

Another factor of successful trophoblast invasion is functional immunology in the area. Normal placentation requires a balance of inhibition and activation of uterine natural killer cells (uNK). This balance depends both on maternal and fetal (Trophoblastic HLA-C) factors.³⁰

Dysfunctional placental apoptosis seems to be another reason of placentation failure and gestosis. Placentas of preeclamptic patients show more apoptotic activity, with increased leakage of syncytiotrophoblast fragments into maternal circulation.^{31,32}

Mammalian placentation requires extensive angiogenesis for the establishment of a suitable vascular network to supply oxygen and nutrients to the fetus. A variety of proangiogenic factors, like VEGF and PIGF, and antiangiogenic factors, such as sFLT-1 and soluble endoglin (sEng), are produced by the growing placenta. The balance of these factors is important for normal placental vascular development, whereas an increased production of antiangiogenic factors tilts this balance and promotes systemic endothelial dysfunction. Several studies have looked into this balance and come to interesting results: One 2010 study showed that low levels of first-trimester PIGF seem to provide a good indicator for IUGR complications and hypertensive disorders, in particular severe cases of pre-eclampsia, such as early onset and HELLP syndrome.³³

In another study in 2008, the antiangiogenic factor sFLT-1 correlated with increasing severity of the disease; sFLT-1 concentrations were higher in women with severe or early (< 34 weeks) pre-eclampsia than in those patients with mild or late pre-eclampsia.³⁴

A study in 2008 from the same research group around, R Romero found that patients who were to deliver an IUGR baby, had higher sEng (antiangiogenic) levels throughout pregnancy than normal pregnant women. When patients were destined to develop preterm and term pre-eclampsia, their sEng levels at 23 and 30 weeks were significantly higher than in normal pregnancies. PIGF (proangiogenic) was significantly lower throughout gestation than in normal pregnancies for women who were to develop IUGR or preterm or term pre-eclampsia. sFLT-1 (antiangiogenic) was no indicator for IUGR, but was significantly higher at 26 and 29 weeks in women who developed preterm or term pre-eclampsia. In conclusion, this indicates that deviation from normal serum levels of sEng, sFLT-1, PIGF preceded pre-eclampsia. Only changes in sEng and PIGF preceded IUGR. In other words, patients with IUGR,

pre-eclampsia, or with both, have different profiles of angiogenic–antiangiogenic factors.³⁵

Another study of this research group in 2010 found that IUFD was characterized by higher maternal serum concentrations of PIGF (proangiogenic) and low sEng (antiangiogenic) during the 1st trimester compared with normal pregnancies. This profile changed into an antiangiogenic one in 2nd and 3rd trimester with low PIGF and high sEng.³⁶

A Japanese study in Feb 2010 showed that the sFLT-1/PIGF ratio in early-onset pre-eclampsia was significantly higher than the one in late-onset pre-eclampsia, suggesting different profiles of angiogenic/antiangiogenic factors for women with early- and late-onset pre-eclampsia.³⁷

In summary, it appears that a practicable approach to a conclusive screening for pre-eclampsia as early as in the 1st trimester could be based on a multivariate evaluation of the following parameters: Maternal history, uterine artery pulsatility index (PI)—increased PI heightens the risk of pre-eclampsia; maternal mean arterial pressure (MAP)—increased MAP boosts the risk of pre-eclampsia; maternal serum concentration of pregnancy-associated plasma protein-A (PAPP-A)—decreased PAPP-A raises the risk of pre-eclampsia; maternal serum level of placental growth factor (PIGF)—decreased PIGF augments the risk of pre-eclampsia.

Factors in the maternal history which require attention, because of their independent contribution to the pre-eclampsia risk include: Maternal body mass index (BMI), age, ethnicity, smoking and parity.

For a 5% false-positive rate, the combination of the above listed risk factors was shown to predict 90% of early onset pre-eclampsia, 35% of late onset pre-eclampsia and 20% of gestational hypertension. This is indeed a remarkable improvement compared with prediction rates of 20 to 30% based on maternal history alone (Fig. 11).^{38,39}

The increased precision of 1st trimester screening has enabled a delectable reduction of unnecessary invasive procedures for fetal karyotyping.

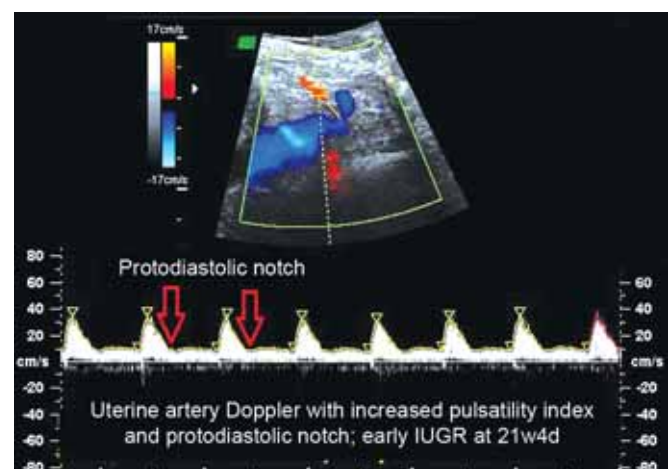


Fig. 11: Uterine artery Doppler

For a more detailed account of theoretical and practical aspects of the 1st trimester screening, the inclined reader is directed to: JD Sonek. First trimester ultrasound screening: An update. *Donald School Journal of Ultrasound in Obstetrics and Gynecology*, April-June 2010;4(2):97-116.

Advances in early assessment of various fetal anomalies. Recent advances of 3D ultrasonography performed with a high frequency transvaginal probe have expanded the depth of sonographic exploration and allowed three-dimensional sonoembryology. Sonographic images can now be obtained of the neural tube of a 6-week embryo, and neurocortical development can be observed in the changing appearance of the Sylvian fissure. Vascular imaging of common and internal carotid arteries, and of the circle of Willis with middle cerebral arteries at 12 weeks is feasible.

Early prenatal diagnosis of anatomical congenital anomalies includes:

- Facial anomalies: Nasal bone, micrognathia, cleft lip
- Vertebral and spinal cord anomalies
- Chest and abdominal anomalies with congenital heart defects (CHD), cystic adenoid lung malformation (CCAM), gastroschisis and umbilical hernia

- Diagnosis of renal and urinary anomalies with posterior urethral valve stenosis at 15 weeks (Figs 12A and B)⁴⁰
- Limb abnormalities: Lethal pterygium syndrome and prenatal diagnosis reported in 1st trimester⁴¹
- Hydrops fetalis: Homozygous alpha 0-thalassemia is the commonest cause of hydrops fetalis in Southeast Asia. The principle of the ultrasound prediction is to detect ultrasonographic features of fetal anemia. Since alpha-globin-dependent hemoglobin F is the major hemoglobin of a fetus from 8 weeks' gestation onward anemia can occur in an affected fetus after reaching this gestational age. Severe anemia and hypoxia result in placentomegaly, fetal cardiomegaly, increased MCA peak systolic velocity, pericardial effusion, ascites and other hydropic features.⁴²

Sonoembryology—new horizons: Transvaginal 3D ultrasound with 12 MHz transducer made it possible to visualize the pre-embryonic period, the embryo and early fetus *in utero*, and thus opened the new field of *sonoembryology* which spans ultrasound assessment of preconception, depicting the cumulus oophorus in preovulatory follicle, assessment of early embryonic development, such as egg division, visualization of perovulatory triple-line endometrium, endometrial and



Fig. 12A: Prune belly syndrome (PBS), incidence of PBS is estimated to be 1 in 30,000 to 50,000 newborn babies



Fig. 12B: PBS at this early stage, key hole sign of dilated proximal urethra, and oligohydramnios are not yet visible

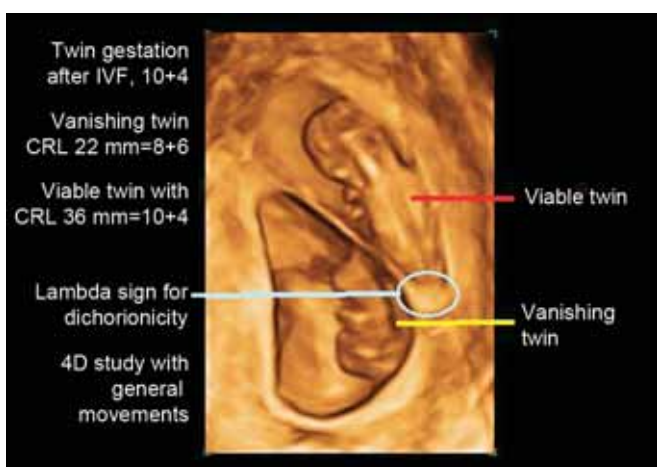


Fig. 13A: Vanishing twin

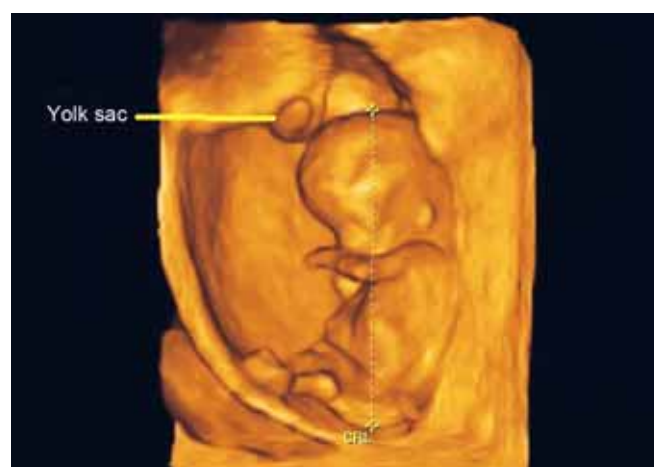


Fig. 13B: Survivor twin

subendometrial blood supply around the time of implantation as determining factors for successful egg implantation, decidual response to invading conceptus as condition for successful trophoblast invasion, and formation of the placenta. Sonographic images can now demonstrate the spinal tube of a 5.5 mm embryo, visualize detailed intracranial structures and embryonic vasculature and enable assessment of thoracoabdominal organs and skeletal elements around 12 weeks.⁴³

Sonographic Visibility Milestones of Embryonic and Early Fetal Development:

- 5 to 6 weeks of gestation: GS, Yolk sac, embryonic blood circulation, vitelline duct circulation, maternal intervillous circulation
- 7 to 8 weeks of gestation: Brain vesicles, development of hand and foot plates, face shaping, abdominal wall and umbilical cord insertion
- 9 to 10 weeks of gestation: Continuation of brain and face development, choroid plexus, physiological umbilical hernia, early spine can be examined at full length, internal fetal vascularity and systolic pulsation in umbilical cord. Lumbosacral myelomeningocele is detectable at this stage.⁴⁴

Three- and four-dimensional (3D, 4D) ultrasound offer new insights into embryonic and early fetal movements and behavior, opening new territories for scientific studies of early fetal neurodevelopment in singleton and multiple pregnancies.⁴⁵

Embryonic reactions to tactile intertwin stimulation have been reported as early as 8 and 9 weeks of gestation.⁴⁶

Vanishing twin phenomenon in monochorionic multiple pregnancy with its hemodynamic implications for the survivor twin bred new hypothesis to explain higher CP-risk for normal birth weight twins compared with singletons (Figs 13A and B).⁴⁷

Three-dimensional Sonoembryology

3D sonography is in several aspects superior to the standard 2D presentation of the 1st trimester pregnancy. Advantages include: Improved assessment of complex anatomic structures, surface scan analysis of minor defects, volumetric assessment of organs, spatial depiction of blood flow information, three-dimensional visualization of fetal skeleton.

During the 1st trimester of pregnancy when exposure to ultrasound should be limited, when manipulation (angling) of the vaginal probe is restricted and when proper sections of fetal structures are sometimes difficult to obtain due to inadequate position of the fetus, a volume sweep taking only a few seconds can provide unlimited tomographic sections, permits rotation of the object to overcome fetal malpositioning, and allows repeated analysis/postprocessing of the stored volume without physical presence of the patient.

Three-dimensional sonography offers two principal modes of imaging: The planar mode and the full 3D image. In the planar mode, the object is simultaneously projected onto three perpendicular planes, the A, B, and C plane (Fig. 14).

All three planes can be separately activated for rotation in x, y and z-axis which offers excellent precision of any

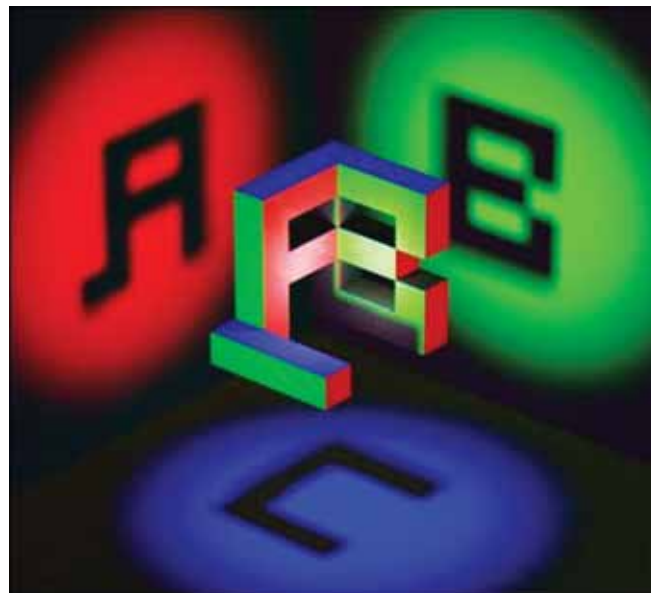


Fig. 14: A, B and C plane (three-dimensional ambigram by Philipp Lenssen)

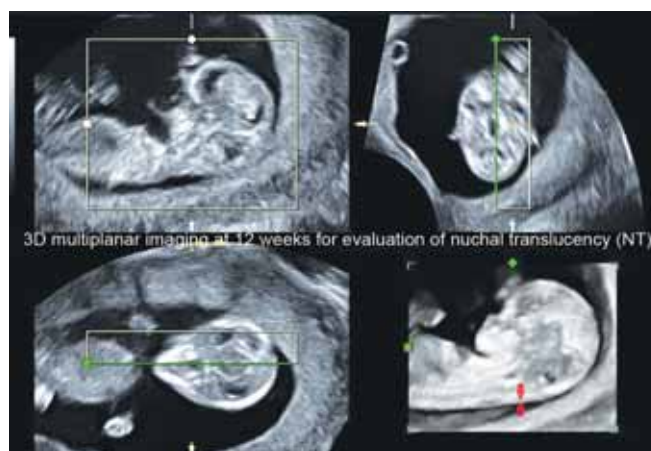


Fig. 15A: First trimester screening 3D assessment of NT



Fig. 15B: First trimester NT-assessment by 3D rendering

measurement. This feature has been shown to be of special value for nuchal translucency measurement when standard 2D approach failed because of unfavorable fetal position (Figs 15A and B).

Full 3D mode may be compared to an anatomic study similar to a vivisection: By moving the rendering line into the object we learn about *in vivo* interrelationship of different organs or the spatial arrangement of the skeleton. This evaluative approach to a stored volume data set can be demonstrated with the example of fetal diagnosis of a Hutch diverticulum. Paraurethral or Hutch diverticula are congenital bladder diverticula that occur at or adjacent to the urethral hiatus and are associated with vesicoureteral reflux (VUR) in the majority of cases. Vesicoureteral reflux is the retrograde passage of urine from the bladder into the upper urinary tract. It is the most common urologic diagnosis in children, occurring in approximately 1 percent of newborns and as high as 30 to 45 percent in children with urinary tract infection (UTI). Current management is based upon the long-held belief that VUR is a risk factor for renal scarring because it predisposes patients to recurrent acute pyelonephritis by transporting bacteria from the bladder to the kidney. The development of renal scarring increases the risk of hypertension and chronic kidney disease (CKD) (Figs 16A to E).⁴⁸

Pulsed wave, color and power Doppler: Adding pulsed wave, color and power Doppler to 3D ultrasound enabled spatial assessment of blood flow within a 3D region of interest (3D-ROI). Only after reaching this new level of diagnostic ultrasound technology, measurements of blood flow and vascularity became possible in the periovulatory follicle and endometrium, and, after ovulation and fertilization, in the region of implantation. As embryonic and chorionic/placental structures develop, their hemodynamic properties become more pronounced and differentiation into a maternal, a placental and an embryonic/fetal unit is now possible on the basis of different flow characteristics.⁴⁹

Events following Implantation

5th week: Gestational sac (GS) visible eccentric within the endometrium, appears as hypoechoic oval structure, surrounded by a hyperechoic ring.

Maternal uterine unit: Gradual decrease of uterine artery resistance index (RI) during the 1st trimester, leveling of the protodiastolic notch, increasing diastolic flow velocities.



Fig. 16A: Paraureteral or hutch diverticula are congenital bladder diverticula that occur at or adjacent to the ureteral hiatus

These changes are consequence of decrease in total peripheral resistance to flow, caused by progressive conversion of spiral arteries into nonmuscular dilated tortuous channels after trophoblast invasion (1st wave of trophoblast invasion). Dilated spiral arteries are easily detected with color or power Doppler close to the chorion, near the placental implantation site and are well recognizable with relatively lower RI and higher peak systolic velocities followed by turbulent flow (Comet sign).

Placental unit: Primary chorionic villi appear during the 4th week of gestation and mark the beginning of placental development. At 5 weeks' gestation, chorionic villi have branched, and mesenchymal cells within the villi have differentiated into capillaries and started to form an arteriovenous capillary network. Until 8 weeks, chorionic villi have covered the entire GS. In the 9th week, on the side of the chorion which has the connecting stalk and embryo, the villi proliferate toward the decidua basalis and form the chorion frondosum, whereas they begin to degenerate on the opposite side, in the area of the decidua capsularis which then transforms into an avascular shell. Normal placentation is characterized by progressive change of spiral arteries into wide channels. The trophoblast carries these changes deep into the inner third of the myometrium, until at the end of 20 weeks gestation all spiral arteries are transformed into wide blood channels (2nd wave of trophoblast invasion). Disturbance of 1st and 2nd trophoblast invasion is suspected to be leading cause of early pregnancy failure and pre-eclampsia.

Pulsed Doppler analysis of intervillous placental flow demonstrates two types of waveforms: Pulsatile arterial-like flow and continuous venous-like flow.

Fetal Unit

Transvaginal approach (5th week): Embryo with attenuated tail and deep neural groove visible. Heart prominence recognizable (Fig. 17).

3D: Gestational sac (GS) visible as small anechoic vesicle placed in one of the endometrial leafs. 3D ultrasound with planar

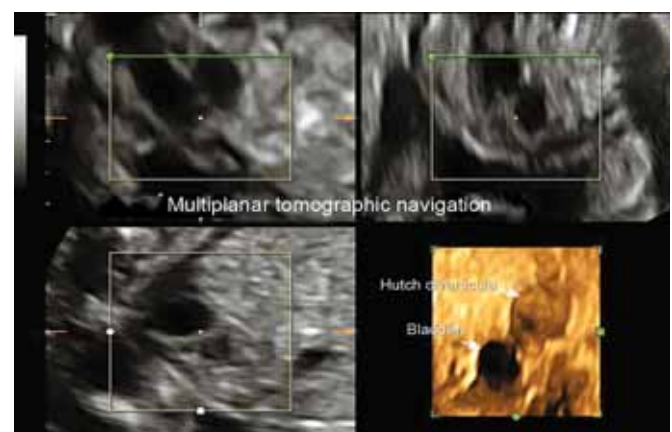


Fig. 16B: Hutch diverticula are associated with vesicoureteral reflux in the majority of cases

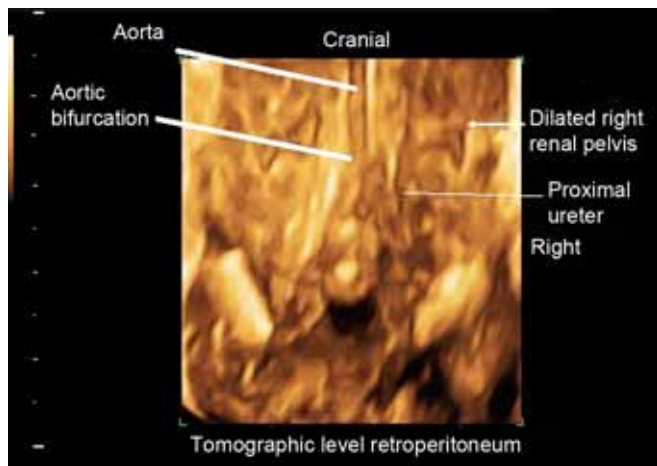


Fig. 16C: Hutch diverticula vesicoureteral reflux (VUR) is the retrograde passage of urine from the bladder into the upper urinary tract

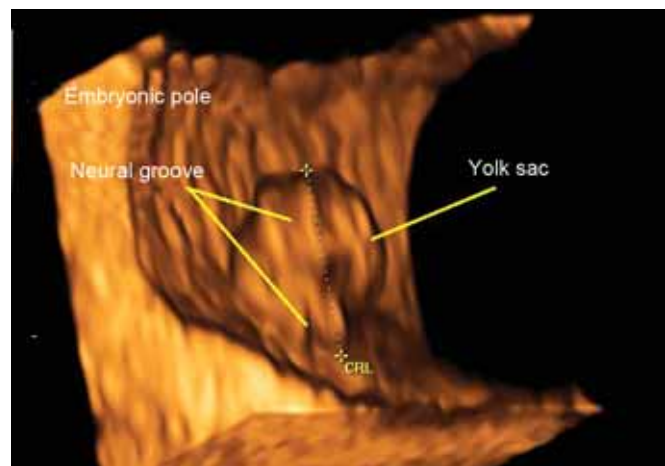


Fig. 17: Embryo 5 to 6w 3D surface rendered GS with embryo and yolk sac

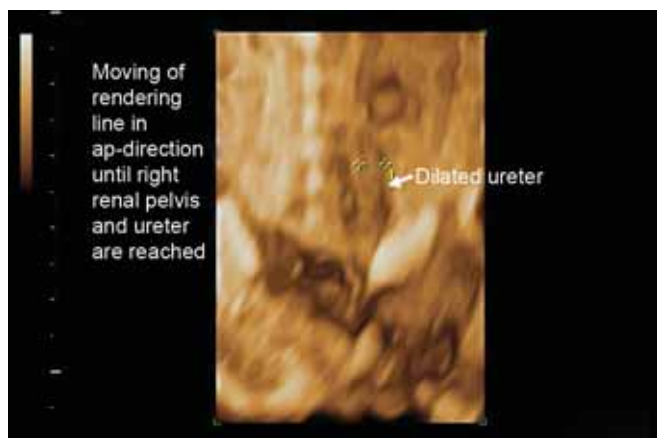


Fig. 16D: Vesicoureteral reflux (VUR) is the most common urologic diagnosis in children, occurring in approximately one percent of newborns

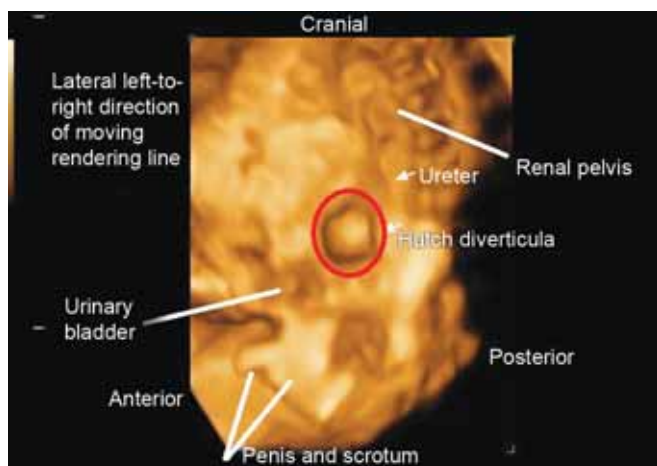


Fig. 16E: Hutch diverticula lateral view

mode at the end of 5th week, at a GS diameter of 8 mm and above, allows easy discrimination of yolk sac and embryonic pole of 2 to 3 mm length, which appears 24 to 48 hours after visualization of the yolk sac, at approximately 33rd postmenstrual day.

3D power Doppler: Intense vascularity around the chorionic shell. The hyperechoic chorionic ring is interrupted by color sprouts of the early intervillous and spiral artery blood flow (Comet sign) (Figs 6A and B).

Transvaginal approach (6th week): C-shaped embryo with dominating head. Physiological midgut herniation begins. Embryonic erythropoietic stem cells, produced at first in the yolk sac and para-aortic mesoderm (aorta-gonad-mesonephros region), have colonized the liver, where erythropoiesis now continues.⁵⁰

3D: Rounded bulky head due to developing forebrain and thinner body, umbilical cord and ductus vitellini discernable. Surrounding the embryo, amniotic membrane with extra-amniotic yolk sac visible. Limb buds are rarely seen at this stage. Ductus omphaloentericus present, with up to four times the length of the embryo.

3D power Doppler: Fetal heart from 5 weeks 4 days onward at crown rump length (CRL) 3 to 4 mm, with heartbeat visible as well, aorta and umbilical cord to placental insertion. Proof of embryonic viability.

Transvaginal Approach (7th week): GS occupies about one third of the uterus. The main landmark is now an echogenic embryonic pole adjacent to a cystic yolk sac. The embryonic head is much larger than the trunk and bent forward over the cardiac prominence. Hand and foot plates are formed, digital rays start to appear. The vitelline duct as part of the vitelline circulation undergoes complete obliteration during the 7th week [in about 2% of cases its proximal part persists as a diverticulum from the small intestine, Meckel's diverticulum, which is situated about 60 cm proximal to the Bauhin's valve (ileocecal valve), and may be attached by a fibrous cord to the abdominal wall at the umbilicus].

3D: Chorion frondosum distinguishable from chorion leave. Amnion visible as spherical hyperechoic membrane, still close

to the embryo. The head has become the dominant embryonic structure. Using 3D planar mode, the rhombencephalon (hind brain), at this stage the largest of the developing vesicles of the brain, can be found at the top of the head (vertex).

3D power Doppler: At the end of the 7th week, cerebral blood flow becomes apparent at the base of the embryonic skull, with discrete pulsations of the carotid arteries. Venous and arterial blood flow signals from the intervillous space have become more intense.

Transvaginal approach (8th week): Transabdominal approach possible (except in retroverted uterus).

CRL 10 to 16 mm: The embryo has developed a skeleton, though still mostly cartilaginous. The head begins to erect from the anterior flexion due to the expansion of the lateral, third and midbrain ventricles. Vertex of the embryo shifted now to the midbrain (mesencephalon).

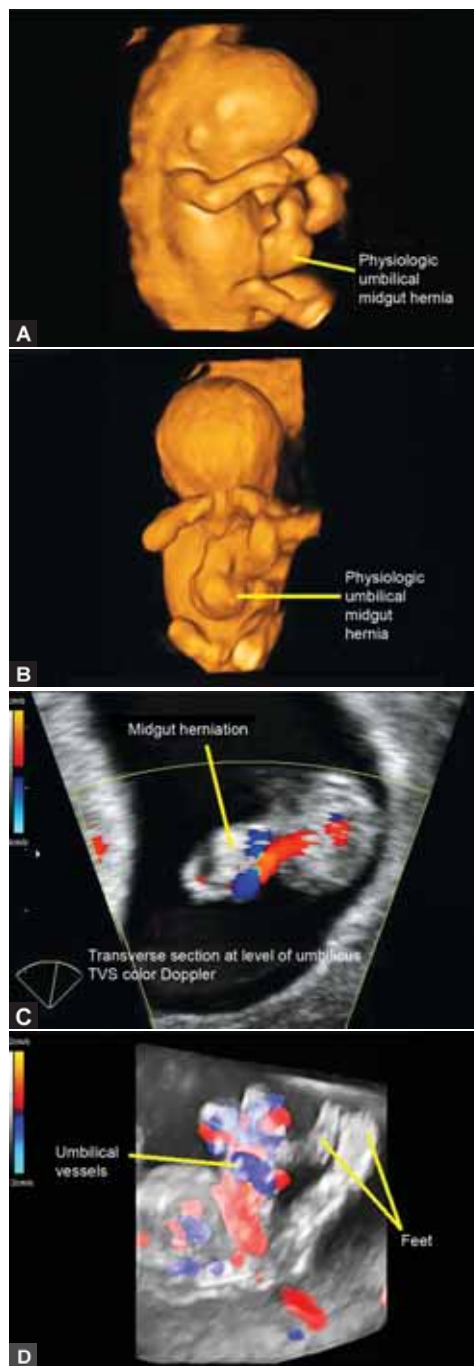
3D: The most impressive change is the complete visualization of the limbs with thickening of the ends where hands and feet develop. The distinction of facial forms is still rather vague, due to insufficient ultrasonographic resolution and because of persisting cranial pole flexion. Umbilical cord insertion visible.

3D power Doppler: At this stage of pregnancy, 3D power Doppler allows the visualization of the entire embryonic circulation (Figs 18A to C).

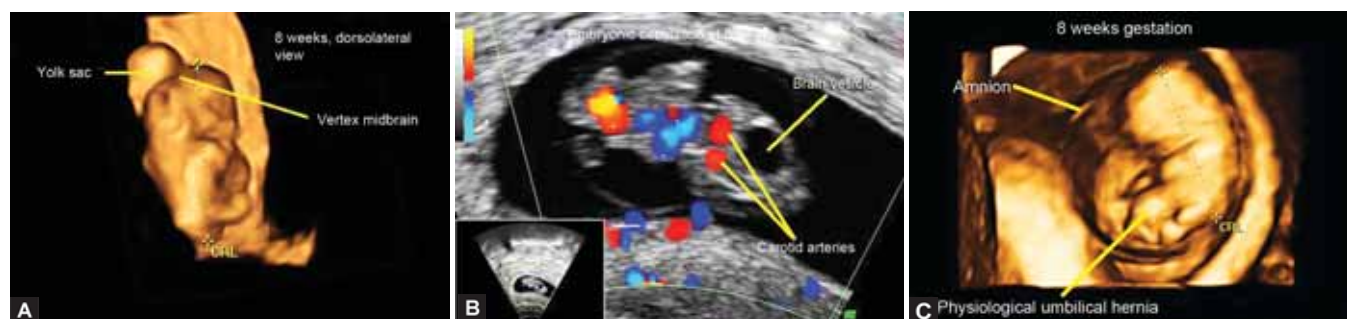
End of embryonic period (9th and 10th week): Transvaginal approach still most accurate, transabdominal approach possible.

The head constitutes now almost half of the fetus. Upper limbs develop faster than lower limbs, formation of fingers complete at the end of 9th week. The rapid growth of the liver and intestine before closure of the abdominal wall may cause herniation into the proximal umbilical cord in most fetuses (physiological midgut herniation). At 10 weeks, when the abdominal wall finishes its development with closure, the bowel undergoes two turns of 180 degrees, with final return to its original position.

3D: Physiological midgut herniation visible. The dorsal column (early spine) characterized by two echogenic parallel lines, can be examined in whole length. The arms with elbows and legs



Figs 19A to D: Umbilical hernia physiologic at 10w5d, (B) umbilical hernia physiologic at 10w5d, (C) umbilical hernia physiologic gray scale CD, (D) umbilical hernia physiologic 10w5d glass body CD



Figs 18A to C: (A) Embryo 8w, beginning erection of the head, foot and hand plates, (B) fetal circulation at 8w with both carotid arteries (C) 8w5d physiological umbilical hernia



Fig. 20: Spinal column at 10w5d, characterized by two echogenic lines

with knees are visible. Head is clearly divided from the body by the neck. At this gestational age, images of the fetal face can be obtained. The lateral ventricles in the brain are seen, containing the hyperechoic choroid plexus (Figs 19A to D and Fig. 20).

3D power Doppler: From the 9th week, the circle of Willis and its major branches are visible.

Transvaginal and transabdominal approach (11th week): Physiological midgut herniation disappears. Fetal kidneys start to produce urine, fetal bladder is visible.

3D: Planar mode enables visualization of the entire fetal body, with differentiation of fetal stomach and urinary bladder. Kidneys become visible. Detailed 3D analysis of the fetal skeleton using maximum mode is possible, the spine is seen in detail. Facial details such as nose, maxilla, mandibles and orbits can be differentiated.

3D power Doppler: Depiction of major aortic branches like renal and common iliac arteries achievable.

Transvaginal and transabdominal approach (12th week): The fetal neck is well defined, the face is broad, with wide distance between the eyes. Structural development of the heart is complete (four chamber view). Erythropoiesis shifts from liver to spleen. Fetal gender can be distinguished.

3D: Depiction of fetal anatomy has reached a degree of accuracy which allows counting of fingers and toes. The growing cerebellum is clearly visible, the lateral ventricles with choroid plexus dominate the brain. From now on, differentiated visualization of vertebral anatomy is feasible using maximum mode: The medullar channel, each vertebra, intervertebral disks, and the ribs can be measured.

3D power Doppler: Fetal vascular system is now part of detailed anatomic survey of cerebrum, digestive and urinary tract. The



Fig. 21A: Early fetal circulation at 12w3d surface rendered fetus

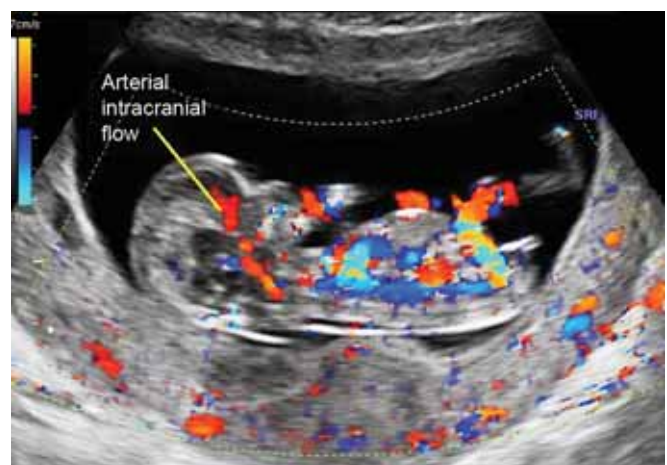


Fig. 21B: Early fetal circulation color Doppler

middle cerebral artery with its pulsations can be differentiated within the circle of Willis. Until the end of the first trimester, the absence of end-diastolic flow in fetal circulation, including umbilical arteries, is a normal finding (Figs 21A and B).⁴⁹

The Yolk Sac

The microscopic structure of the primary yolk sac is visible in an implanted 9 days human blastocyst and extends as a cavity surrounded by the exocoelomic (Heuser's) membrane and the cytotrophoblast layer toward the not yet completely closed surface defect of the endometrium at the site of implantation. At the base (embryonic pole) of the primary yolk sac is the inner cell mass, the embryoblast. Beyond the embryoblast and the small half-moon shaped early amniotic cavity, toward deeper layers of the endometrium, follows a thicker cell layer of cytotrophoblast, and the syncytiotrophoblast. Here is the future location of the embryonic stem and the chorion frondosum as the main area of trophoblast invasion into maternal spiral arteries. Between the exocoelomic membrane (Heuser's) and the cytotrophoblast develops until day 12 postconception a surrounding layer of fluid creating the extraembryonic coelom, also called chorionic cavity. The primary yolk sac, being now

surrounded by the extraembryonic coelom, has hence become the secondary yolk sac, visible until about 12 weeks of gestation. The secondary yolk sac is by origin embryonic tissue and ultrasonographically the first visible embryonic structure in the GS at 5 weeks: It appears as circular, well-defined, echo-free area, diameter 3 to 4 mm, within the GS which measures at this time about 8 to 10 mm. The yolk sac grows slowly until it reaches a maximum diameter of approximately 5 to 6 mm at 10 weeks. Its stalk (vitelline duct) can be followed from the origin into the embryonic abdomen. The vitelline duct is a tubular elongation connecting yolk sac and embryonal midgut which had developed during progressive separation of the yolk sac from the embryo through formation of the intraembryonic body cavity, with the embryonic stalk as remaining opening. The yolk sac is the source of omnipotent stem cells including the gametes which are formed from primordial germ cells in the embryoblast and which later move into the wall of the yolk sac. From here, they migrate through the vitelline duct into the embryo. As the gestational sac grows and the amniotic cavity (the yolk sac was always extra-amniotic) quickly expands, the yolk sac as 'extra-embryonic' structure is gradually separated from the embryo (Fig. 22A).

Anomalies of the Yolk Sac

The following changes assessed by 2D US are related to subsequent spontaneous abortion: Absence of yolk sac, enlarged yolk sac (more than 6 mm), too small yolk sac (less than 3 mm), irregular, wrinkled shape of yolk sac with indented walls, degenerative changes of the yolk sac such as abundant calcifications with decreased translucency of yolk sac, and abnormal number of yolk sacs which normally has to be equal to the number of the embryos. Currently, the major benefits of a sonographic evaluation of the yolk sac are as follows: Differentiation of potentially viable and nonviable gestations—indication of a possible embryonic abnormality. Abnormal small size of the yolk sac and increased echogenicity have been shown to be markers of poor pregnancy outcome (Fig. 22B).⁵¹

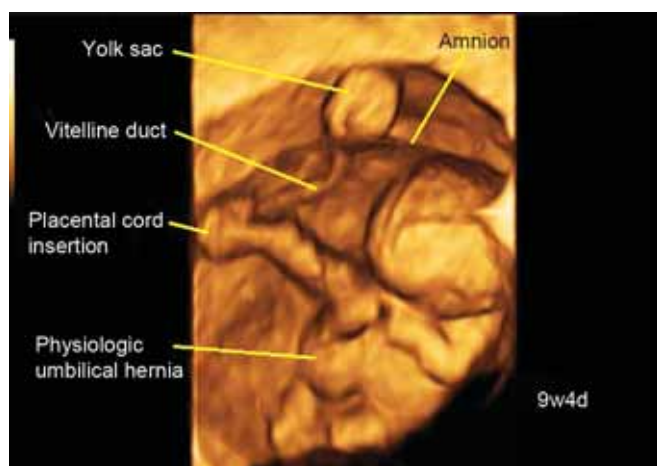


Fig. 22A: 3D surface rendering relation of amnion and yolk sac, 9w4d

Scientific evaluation of yolk sac and vitelline duct as first visible signs of embryonic presence is fascinating. However, there should be awareness of potential damage to erythropoietic stem cells and germ cells by Doppler and especially pulsed Doppler application in this stage of embryonic development, in this area. The knowledge about yolk sac vascularity and vitelline duct flow profiles was, therefore, collected from 150 patients about to undergo termination of pregnancy for psychosocial reasons.⁵²

The most intense visualization of yolk sac vessels was around 7 to 8 weeks of gestation (5-6 weeks postconception), with a sharp decline hereafter due to ceasing vitelline circulation (obliteration of vitelline duct around 7th week of gestation). A characteristic flow waveform in all examined yolk sacs included low velocities and absent diastolic flow, with a mean pulsatility index (PI) of 3.24. The authors found a positive correlation between gestational age and yolk sac volume until 10 weeks. At the end of the 1st trimester, the GS volume continued to increase while the yolk sac remained the same. Kurjak et al coworkers also analyzed yolk sac vascularization in abnormal pregnancies.⁵³

Flow signals were detected in 18.54% of 48 patients with the diagnose 'missed abortion' between 6 and 12 weeks gestation. Three types of abnormal flow signals could be observed: Irregular blood flow, permanent diastolic flow and venous blood flow type. Because nutritive secretions of the yolk sac are not utilized by the deceased embryo, dysfunctional vitelline circulation could result in insufficient drainage of the yolk sac with progressive accumulation of contents. Consequently, an increased yolk sac volume indicates early pregnancy failure. An embryonic heart rate less than 100 beats per minute (bpm) before 7 weeks is considered as embryonic bradycardia. Bradycardia or arrhythmia often predict subsequent heart action cessation. Such cases of early hemodynamic heart failure usually go along with yolk sac enlargement (more than 6 mm) and initial generalized hydrops.⁵³



Fig. 22B: Triplets, hyperechoic yolk sacs, one week before spontaneous miscarriage

Multiple Pregnancy

Determination of chorionicity and amnionicity in multiples is one of the important goals of early pregnancy ultrasound, because of its prognostic value in regards to subsequent development of discordant growth or/and twin-to-twin transfusion syndrome (TTTS). 3D surface rendering of multiple gestation is an excellent



Fig. 23A: Lambda sign in triplets



Fig. 23B: T-sign in monoamniotic twins



Fig. 24: Triplets dichorionic diamniotic and monoamniotic with birth weights at 35w

tool because the offline evaluation of the sweep volume will give quick evidence of the number of embryos, their spatial relation, and lambda- or T-sign of separating membranes (chorionicity) (Figs 23A and B and Fig. 24).

Abnormalities in twins can be classified in those specific for monochorionicity, and malformations equally affecting multiple and singleton pregnancies, such as cardiac or neural tube defects. Conjoined twins in monochorionic pregnancies occur when the division of the zygote is delayed until day 13 to 16 postconception (Figs 25A and B).

Early Sonographic Diagnosis of Fetal Anomalies

Congenital heart defects (CHD) have an overall incidence of about 1% in liveborn infants and account for 20% of all stillbirths and 30% neonatal deaths due to congenital anomalies. The etiology of CHD includes maternal diseases, such as diabetes mellitus, phenylketonuria, exposure to substances (anticonvulsants, lithium), infections (parvovirus, rubella), chromosomal anomalies (trisomy 21,18) and specific mutant gene defects. However, there are many unknown causes. The aneuploidy risk for a fetus with CHD is 30%.^{54,55}

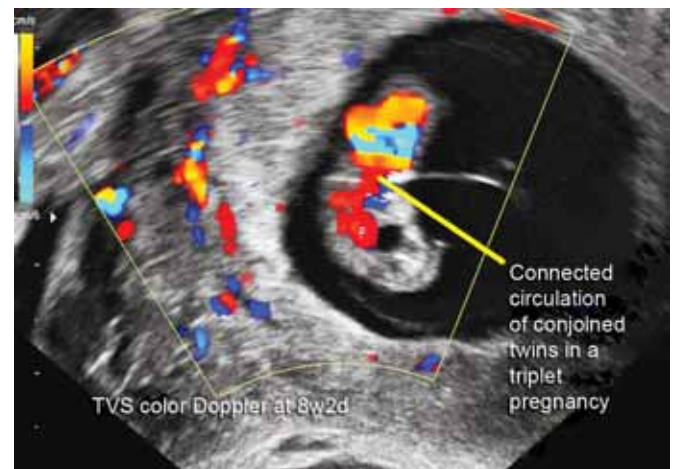


Fig. 25A: Conjoined triplets



Fig. 25B: Conjoined twins in triplet pregnancy, ectopia cordis

The recurrence risk of cardiac anomalies in the absence of a known genetic syndrome is 2 to 4%, and with two previously affected siblings, it is 10%.⁵⁶

CHD, classified as major, have an estimated prevalence of 4 in 1000 live births and are either lethal or require surgical repair or interventional catheterization within the 1st year of life.⁵⁷

It is self-explanatory that CHD should be discovered at the earliest. By the end of the 1st trimester, the period of organogenesis is completed. The cardiovascular system originating from the mesodermal germ layer appears in the middle of the third week. The developing heart tube bends on day 23 and is organized in segments, creating the heart loop. The primitive left and right ventricles begin to expand by the end of the 4th week. During the 4th to 8th week, the formation of the ventricular and atrial septa is complete, and the arterial and venous connections are established. The division of the heart into a four-chamber structure is now achieved. Already 16 years ago, using a high-resolution transducer of 6 to 15 MHz, it was, at this gestational age, possible to obtain satisfactory images of the four-chamber view (FCV) and the outflow tracts in the majority of fetuses.⁵⁸

However, there are critical limitations to a successful early evaluation of the heart, such as experience of the operator, up-to-date technological equipment and length of examination time.

Early Fetal Echocardiography at the Time of 11+0 to 13+6 Weeks

EFE is a highly specialized scan performed until 16 weeks of gestation under exceptional indications like increased nuchal translucency (NT) measurement, congenital heart defect (CHD) risk factors or early diagnosed extracardiac fetal abnormalities. EFE makes sense considering the fact that the severest CHDs do not develop from a normal looking heart, and that equally abnormal sonographic views of such a severely dysmorphic heart can be obtained in the first, second and third trimester. The earliest opportunity for successful fetal heart assessment is offered after embryological finalization of structural heart development at 9w6d postmenstruation (pm). Practically, however, EFE starts at 11 weeks pm. Second trimester fetal echocardiography protocol can be successfully adopted for EFE because the fetal heart at 1st trimester screening is, though smaller, structurally equal to the 2nd trimester heart. Recent publications support the applicability of spatial temporal image correlation (STIC) for EFE.⁵⁹

Indications for EFE: Next to maternal indications which are the same as for midgestational fetal echocardiography, it is mainly the spectrum of findings during nuchal translucency screening which gives reason for EFE: Early diagnosis of malformations with possible association of CHD, such as single umbilical artery, omphalocele, increased NT-measurement, tricuspid valve regurgitation and reversed ductus venosus A-wave (Figs 26A and B).^{60,61}

Since the 1990s, extensive studies have established that euploid fetuses with increased nuchal translucency (NT) have

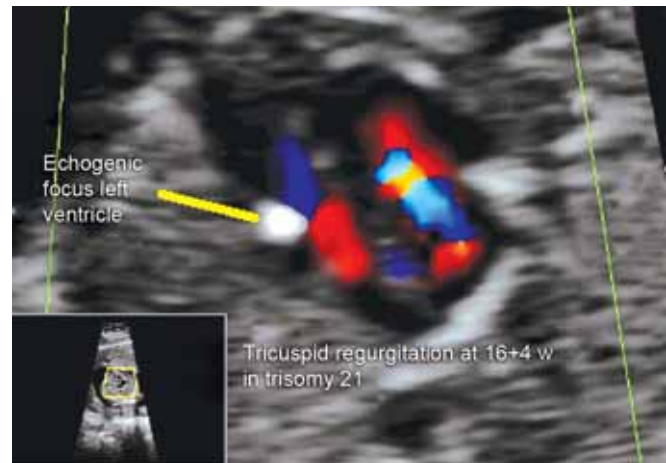


Fig. 26A: Tricuspid regurgitation

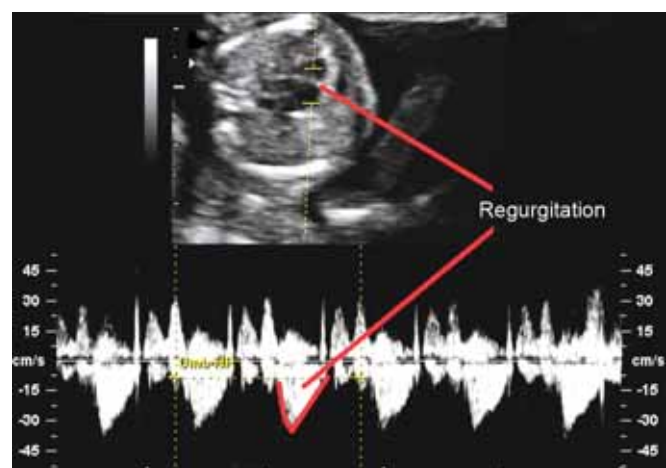


Fig. 26B: Tricuspid regurgitation in trisomy 21 at 16w

a higher risk for a wide range of fetal structural defects, for specific genetic syndromes, and especially for congenital heart defects (CHD).^{62,63}

Severe CHDs with high probability of detection by EFE: D- and L-transposition of the great arteries (D-TGA, L-TGA) hypoplastic left heart syndrome (HLHS) based on aortic and mitral valve atresia or severe stenosis; atrioventricular septal defect (AVSD); double outlet right ventricle (DORV); common arterial trunk (CAT); double inlet left ventricle (DILV); tricuspid atresia (TA); mitral atresia (MA); pulmonary atresia (PA); heterotaxy syndromes; total anomalous pulmonary venous return (TAPVR); large ventricular septal defects (VSD).

Less severe CHDs which may be overlooked when performing EFE: Coarctation of aorta; mild aortic or pulmonary stenosis; mild tricuspid and mitral valve anomalies; cardiac tumors; cardiomyopathies; septal defects, including ventricular atrioventricular and atrial septum primum defects; tetralogy of fallot with normal pulmonary artery size or abnormal pulmonary venous return.^{64,65}

Further detailed information about requirements for EFE with transabdominal and especially transvaginal approach,

image optimization, effectiveness and limitations of EFE may be found in: Wiehac M, Nocun A, Beithon J. Early Fetal Echocardiography at the time of 11+0 to 13+6 Weeks Scan. Donald School Journal of Ultrasound in Obstetrics and Gynecology, July-September 2009;3(3):75-81.

Fetal abdominal wall defects: Fetal abdominal wall defects have an incidence of 17 to 22 per 100,000 live births. The most frequent forms are gastroschisis (1:10,000) and omphalocele (1:10,000), followed by body stalk anomaly (1:14,000 to 42,000), cloacal and bladder extrophy (1:25,000 to 50,000), and pentalogy of Cantrell (1:65,000 to 200,000).⁶⁶

Since ventral wall defects lead to elevated levels of alpha fetoprotein (AFP) in maternal serum (and amniotic fluid), detection of increased AFP concentrations should result in careful sonographic evaluation of the fetal abdominal wall. The antenatal diagnosis of surgically correctable anomalies is very stressful for the parents; however, the delivery outcome of infants with isolated abdominal wall defects benefits clearly from prenatal diagnosis and delivery in tertiary center with pediatric surgery, and the long-term prognosis is generally quite good.⁶⁷

Gastroschisis (Greek: Gastric cleft): Gastroschisis and omphalocele can be seen with ultrasound and are diagnosed after 11 weeks of gestation, when transient structural alterations of the embryo and early fetus like physiological extra-abdominal herniation of the bowel are normally no longer present. While omphalocele is frequently associated with chromosomal abnormalities, gastroschisis is mostly sporadic and bears low risks for chromosomal and extragastrintestinal anomalies.⁶⁸

The ultrasound diagnosis relies on the demonstration of herniated visceral organs adjacent to the anterior abdominal wall and the dilatation of intra-abdominal proximal bowels. The location of the abdominal wall gap is usually to the right of the normal umbilical cord insertion (site of the transient right umbilical vein with involution at day 28 to 32 postconception). The herniated bowels are not covered by parietal peritoneum and float freely in the amniotic fluid.⁶⁹

Color Doppler and 3D ultrasound facilitate the diagnosis by orientating the sonographer about spatial relation between abdominal umbilical cord insertion and extrusion site of bowels (Figs 27A and B).

Omphalocele: Association with other malformations is found in up to 74% of cases, and most commonly, in up to 50% of affected fetuses, with congenital heart defects (CHD), such as ventricular septum defect (VSD), atrial septum defect (ASD) and coarctatio aorta (CA). Aneuploidy is more likely in smaller omphaloceles than in the larger ones. The most common type of aneuploidy is trisomy 18 (Edwards S), less common are trisomy 13 and Turner Syndrome. If the liver is herniated, cardiac, renal and limb anomalies are more frequent.⁷⁰

Color and power Doppler aid in diagnosis by depicting umbilical arteries and umbilical vein in their spatial relation to the omphalocele. Cord vessels are circling the omphalocele and liver topography can be disclosed with electronic scalpel (Figs 28A and B).

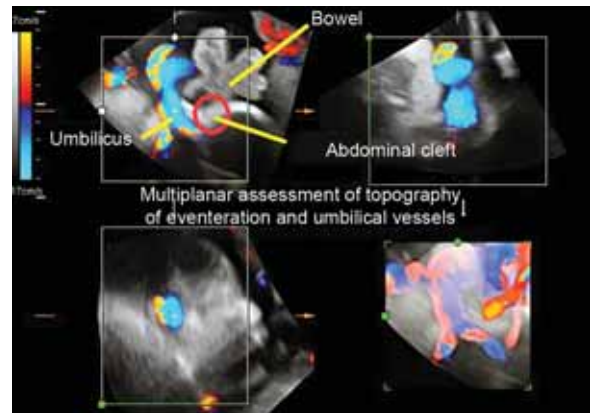


Fig. 27A: Gastroschisis—multiplanar 3D CD

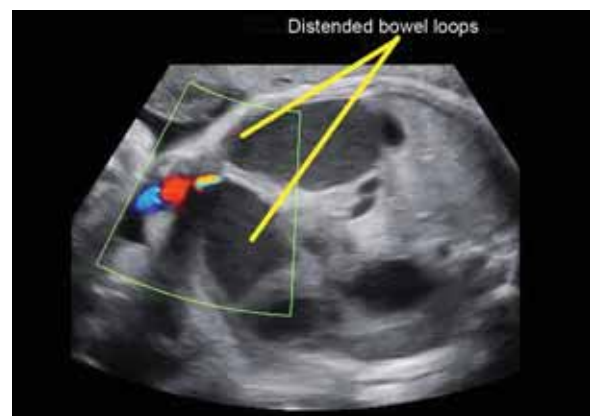


Fig. 27B: Gastroschisis—ileus and umbilical cord location



Fig. 28A: Omphalocele—whole fetus 3D, umbilical vessels joining on top of the omphalocele

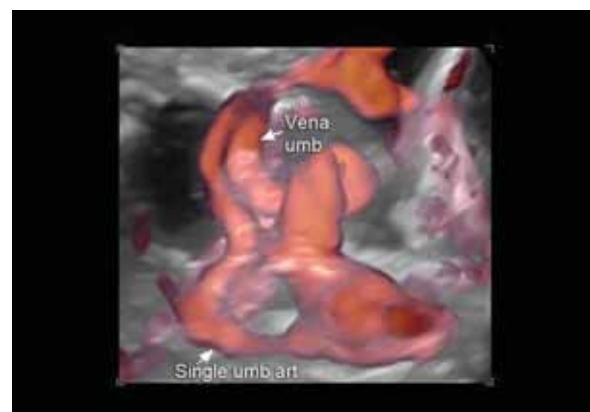


Fig. 28B: Omphalocele—glass body power Doppler

Bladder exstrophy and cloacal extrophy: In both entities, a ventral body wall defect with exposure of the bladder mucosa is present. Sonographic diagnose is possible only near 12 weeks of gestation, after definitive formation of the kidney from the metanephros and onset of urinary production, with filling of the fetal bladder, and excretion of urine into the amniotic fluid. Characteristic sonographic finding after 12 weeks is the repeated absence of a filled bladder in the area between the ventral pelvic curving of the umbilical arteries in color and power Doppler mode (Fig. 29).

Complex Anomalies associated with Abdominal Wall Defects

Body stalk anomaly (alias Limb-Body Wall Complex): Ultrasonic findings at the time of 1st trimester screening may reveal increased nuchal translucency, left lateral thoraco-abdominoschisis and attachment of the fetus to the placenta or uterine wall. At 12 weeks, higher incidence of 1:7,500 fetuses was described.⁷¹

Other anomalies, such as partial or complete limb absence, midfacial clefts, and exencephaly or encephalocele, may be found as well.

Pentalogy of Cantrell: Complex ventral body wall defect with possible association of sternal cleft, ectopia cordis, omphalocele, and anterior (Morgagni) congenital diaphragmatic hernia (CDH) eventually diverse congenital heart defects (CDH). Lack of fusion of the bilateral bars of mesoderm responsible for formation of the ventral body wall at the end of the 3rd week of embryonic development, is considered to be the cause.⁵⁰

Sonographic diagnosis is feasible around 10 to 11 weeks of gestation. However, the variable severity of the malformation might make early diagnosis a difficult task.⁷²

OEIS complex (omphalocele, exstrophy, imperforate anus, spinal defect): Sonographic diagnose of each of the included malformations has already been discussed. The anomaly has sporadic incidence and is—if not lethal—associated with considerable morbidity.⁷³



Fig. 29: Umbilical arteries circling the bladder PD

Early Fetal Neurodevelopment

Sonoembryology of facial development: The human face differs in each individual, its formation is embryologically complex, and growth and remodeling are not complete until postpuberty.^{74,75}

The same inductive forces that cause growth and shaping of the neural tube, influence the development of facial structures. A large number of fetal face anomalies which can be seen using two- and three-dimensional ultrasound techniques are linked with different brain anomalies. It is, hence, correct to say that 'the face predicts the brain' or is the 'mirror of the brain'. While the study of various fetal facial expressions in late pregnancy by four-dimensional ultrasound has become a fascinating part of the new field of fetal neurosonography, early pregnancy ultrasound evaluation of the face is limited to structural aberrations and often hampered by technical limitations like insufficient ultrasonographic resolution of the embryonal face or the predominant flexion of the cranial part of the embryo (hidden face). Behavioral 4D studies of the face at this stage would be probably meaningless due to the immaturity of both midbrain (controlling cranial nerves 3-6, auditory and visual systems) and nuclei of facial nerves 5 and 7 (responsible for motoric facial innervation). From the 9th week on the head is clearly divided from the body by the neck. In the weeks 11 and 12, structures, like the nose, orbits, maxilla, mandible and mouth, can be observed. Around the 13th week, the anatomy of the face is developed and can be analyzed for diagnostic purpose.⁷⁶

Early Fetal Neural Activity

Dealing with structural development of CNS only does not answer the challenging question: What is the neurobiological basis of early fetal movement patterns? In humans, an endogenous neural cortical network is already present at 8 weeks postconception, i.e. at the end of the embryonic period. It contains very few synapses, and it is likely that neuronal communication happens largely through intercellular junctions. Such early neuronal networks display a characteristic oscillatory activity. It is unlikely that these nonsynaptic cortical networks could generate directly early fetal movements; however, their oscillatory endogenous activity might trigger networks in other parts of the brain and spinal cord. From a neurodevelopmental view, these endogenous neuronal activities seem to shape the subsequent process of synaptogenesis.⁷⁷

Embryology of the Human Brain

The neural tissue of brain and spinal cord differentiates from the ectodermal layer of the embryonic disk during the second week of embryonic life (days postfertilization). The ectodermal tissue thickens and forms the symmetric neural plates which are the forerunners of the brain and the spinal cord.

Day 18: A groove appears in the midline of the embryonic disk, becoming deeper and longer due to the elevation of neural folds along both sides of the groove.

Day 20: Thickenings in the cranial neural plate indicate the formation sites of the three sections of the embryonic brain: The primary brain vesicles rhombencephalon, mesencephalon and prosencephalon.

Day 22: The bilateral neural folds begin to fuse with each other, starting simultaneously at three initiation sites:

1. Cervical fusing toward the posterior (caudal) neuropore
2. At the mesencephalic/rhombencephalic boundary fusing toward the anterior neuropore
3. At the rostral end of the neural groove.

Day 24: Anterior and rostral section of neural tube closed

Day 28: Caudal end of the neural tube closed

If the process of fusion is disturbed, various forms of neural tube defects (NTD) can occur.

After day 28: Soon after the closure of the neural tube, the three sections of the embryonic brain undergo a process of flexion. The prosencephalon divides into an end portion called telencephalon from which the future cerebral hemispheres originate and into the diencephalon from which bilateral optic vesicles arise. The rhombencephalon divides into a rostral part, the metencephalon, and a caudal part, the medulla oblongata. From 9 weeks onward, then follow the formation of the cerebral hemispheres, the interhemispheric connections, in particular corpus callosum, the development of the cerebellum, and the sculpturing of brain lobes, sulci and gyri.

After 6 weeks, migration of neurons: Until now homogeneous neuroepithelial tissue of spinal cord and brain begins to form into several histologically recognizable zones: The ventricular zone filled with ventricular cells and dividing neural precursor cells. It is in the ventricular zone, where the cortical neurons are generated who are destined to migrate through the other zones along associated glia cells up into the cortical plate.

After 8 weeks, myelination: For proper conduction of neuronal impulses, axons of neuronal cells need to undergo myelination. In the central nervous system (CNS), myelination is performed by oligodendrocytes. Myelination is a slow process, which begins in the brainstem at 8 weeks, finishes in the vestibulospinal tract at the end of the 2nd trimester, and begins in the pyramidal tracts only at the end of the 3rd trimester, thus explaining the relative immaturity of the human brain at the end of gestation.^{78,79}

Spinal cord: The spine is formed between 20 and 30 days of gestation in a process called somitogenesis. In the developing vertebrate embryo, somites are masses of mesoderm distributed along the two sides of the neural tube that will differentiate into dermis (dermatome), skeletal muscle (myotome) and vertebrae (sclerotome). The somites are sized and spaced regularly. Since Gray et al in 1991 evaluated the ossification pattern of the vertebra by ultrasound, it is known that there are separate ossification centers for the vertebral body and for each of the neural arches. The ossification of the neural arches occurs in a predictable pattern, proceeding in caudal direction, progressing

from L2 downward, with ossification of one vertebral level every 2 to 3 weeks, until S2 is ossified by 22 weeks.^{80,81}

In the embryonal period, the CNS develops faster than other embryonic structures, whereas in the subsequent fetal period, the vertebral column grows faster than the spinal cord.

Positional Changes of the Spinal Cord

Around 12 weeks of development, the spinal cord extends the entire length of the embryo, and spinal nerves pass through the intervertebral foramina at the level of their origin. However, with increasing gestational age the vertebral column and the dura mater lengthen faster than the neural tube, sort of leaving the neural tube behind, and the terminal end of the spinal cord gradually shifts to a higher level. At birth, this end is at the level of the 3rd lumbar vertebra. Below L3, a threadlike extension of the pia mater surrounding the spinal cord forms the filum terminale, which is attached to the periosteum of the 1st coccygeal vertebra. Spinal nerve fibers passing through foramina intervertebralia below L3, gradually have to extend with the accelerated growth of the vertebral column, and collectively constitute the cauda equina within the vertebral channel at the end of gestation (Figs 30A and B).⁵⁰

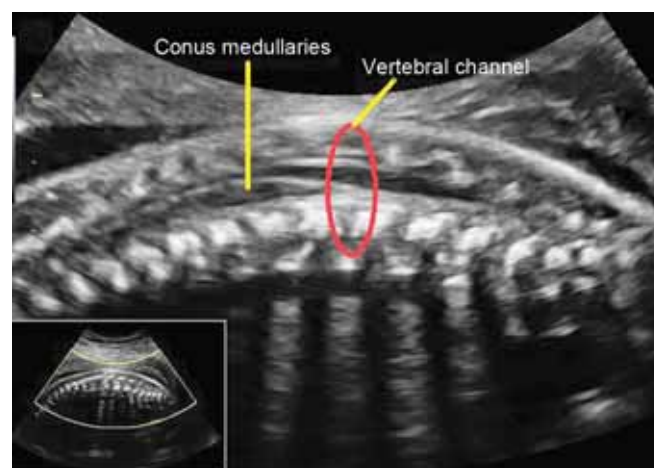


Fig. 30A: Vertebra at 26w B-mode conus medullaris



Fig. 30B: Vertebra at 26w orthogonal view into vertebral channel 3D

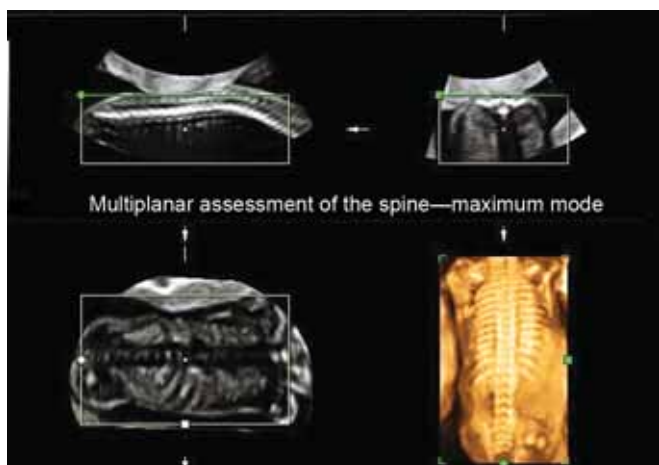


Fig. 31: Multiplanar sections vertebra

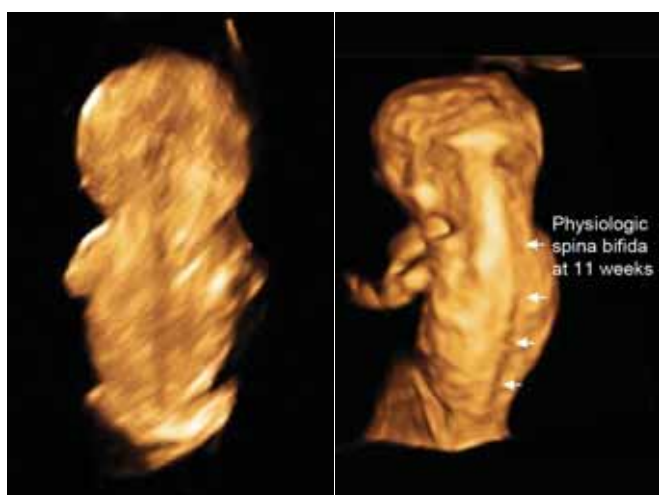
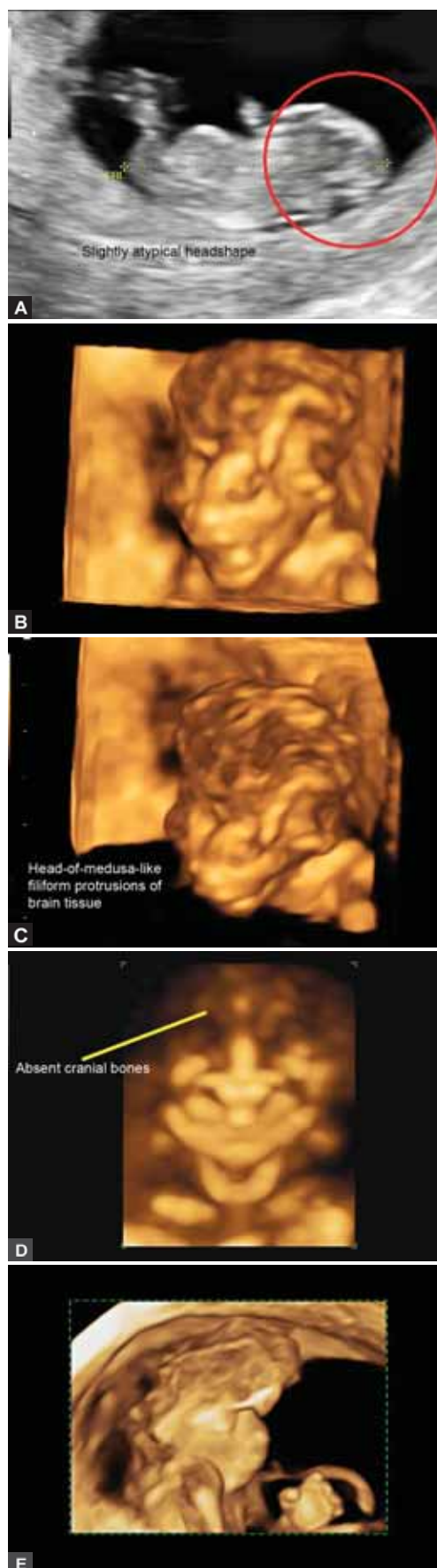


Fig. 32A: Physiologic spina bifida at 9 weeks Fig. 32B: Physiologic spina bifida at 11 weeks

With 3D ultrasound, by moving the region of interest (ROI), 3D reconstruction image of the surface level, neural arch level and vertebral body level of the vertebral column is possible. By 13 weeks of gestation, vertebral bodies, intervertebral spaces and bilateral premature arches can be clearly demonstrated (Fig. 31).

Until 15 weeks, the bilateral lamina of the neural arches are still completely apart at all levels of the vertebral column, but at the lumbosacral level, the median gap between the bilateral neural arches is wider than at thoracic level. This stage of development is called ‘physiological spina bifida’ (Figs 32A and B).

Neural tube defects (spina bifida) are classified into four types: Meningocele, myelomeningocele, myelocystocele, myeloschisis. In myelomeningocele, the spinal cord and its protective covering, the meninges, protrude from an opening in the spine. In meningocele, only the meninges protrude from the spinal gap, whereas the cord is in normal position. The lumbar and sacral levels of the vertebra are the most common locations. Early detection by 2D and 3D imaging of spina bifida with meningomyelocele at 9 weeks, and at 10 weeks in combination with iniencephaly and acrania, was described by Pooh RK and Kurjak A in 2008 (Figs 33A to E).



Figs 33A to E: (A) Acranium 10w in B-mode, (B) acranium 12w 3D surface rendered face, (C) acranium 12w brain tissue, (D) acranium 12w maximum mode head AP, (E) acranium-head and hand 3D at 17w4d open fingers normal position of the thumb

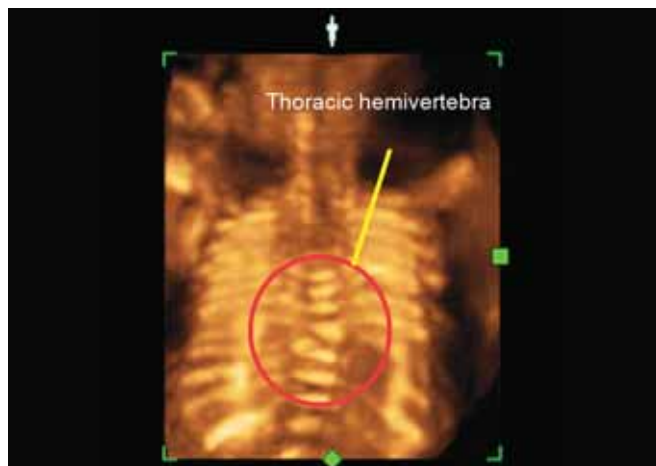


Fig. 34: Hemivertebra multiplanar maximum mode

Prevalence is 0.7 to 2/1000 births. As etiological factors, single mutant genes, autosomal recessive inheritance, chromosomal aberrations (trisomia 13, 18), folic acid antagonists, enzymatic defects in folic acid metabolism, specific teratogens like valproic acid, maternal diabetes and environmental factors are evidently or suspected responsible.

As described previously, the spine is formed between 20 and 30 days of gestation in a process called somitogenesis. A disruption of the drastic cellular cytoskeletal rearrangements and biochemical changes can result in hemivertebra and congenital scoliosis (Fig. 34).

Dynamic Real-time 3D Ultrasound (4D) and Fetal Behavior in Early Pregnancy

3D surface rendering of embryonic and fetal structures has been a huge step forward in prenatal sonographic diagnosis. The rapid succession of 3D surface rendered images of a ROI, with frequencies of up to 40 Hz and sufficient image quality and volume angle, is called dynamic real-time 3D (4D). This ultrasound mode opened many doors to new research fields, one of them the study of fetal neurobehavior: It enables the sonographer to appreciate not only embryonic and fetal posture and typical (repetitive) patterns of movement, but also abnormality, lack or absence of such movements. Human fetuses, and in continuation, newborn children up to the age of four months post-term, have distinct patterns of spontaneous, not externally triggered movements, called general movements (GM) which were defined by Prechtl⁸² as gross movements, involving the whole body and lasting from few seconds to several minutes, or longer. GMs can be described as a variable sequence of arm, leg, neck and trunk movements, which begin gradually, increase in force and speed, and then slacken down again. Extension and flexion movements of arms and legs are mostly complex and variable due to integrated rotations and frequent minor changes of direction, which adds a fluent and elegant quality to the movements. GMs follow after the early embryonic vermicular movements and are first seen from 8 weeks of gestation onward. The nature of the recognizable

temporal sequences of GMs lies in the intrinsic properties of neurons which spontaneously begin to generate and propagate action potentials on their own, and this even more as soon as they are interconnected. This action potential generating neuronal network for the initiation of GMs could be primarily located in the spinal cord and the brainstem which consists of medulla oblongata, pons and midbrain. The development and maturation of the fetal CNS in the 2nd and 3rd trimester is characterized by synaptogenesis and myelination. By 20 weeks, the cerebral cortex has acquired its full complement of neurons. The first evoked potentials from the cortex can be registered at 29 weeks; however, until delivery and neonatal period, subunits of the brainstem remain the major regulators of all movement patterns of the fetus and neonate⁸³⁻⁸⁵ and thus maintain their signature on fetal and neonatal behavior.

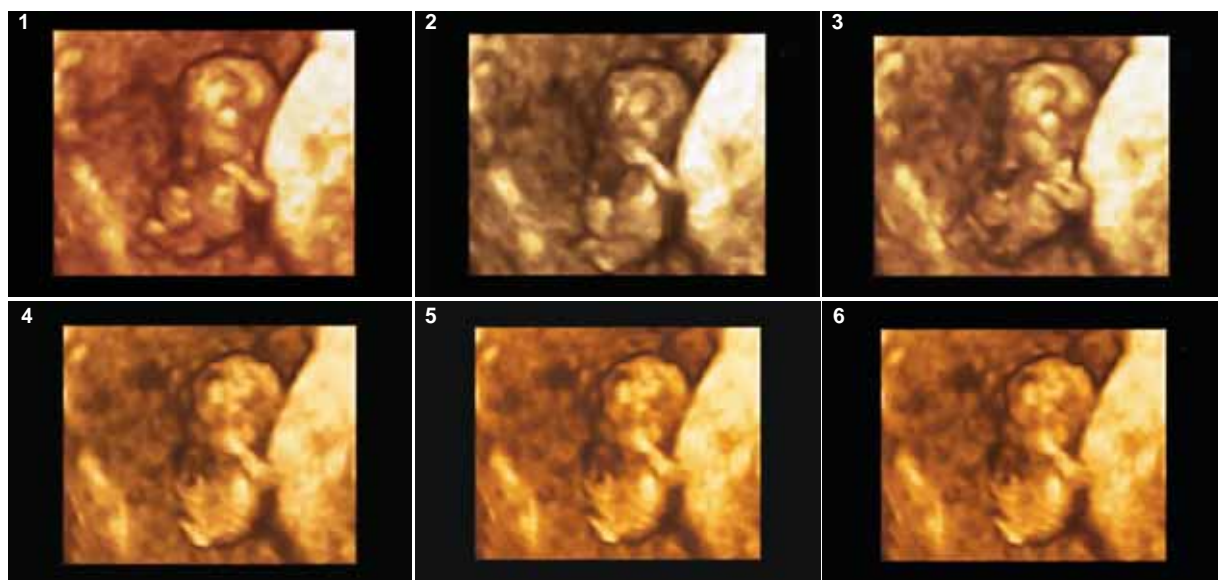
Assessment of fetal behavior in different periods of gestation promises recognition and early diagnosis of abnormal brain development and various structural and functional CNS abnormalities.⁸² With the advent of 4D or real-time 3D ultrasound, straightforward visual transfer of fetal GMs to the sonographer's eye has become possible. The human eye can differentiate single images up to a frame rate of 12 Hz, above this frame rate, serial images are perceived as continuous movement. Presently, peak frame rates in high-end equipment reach 40 Hz. This enables visualization of even small facial twitches of the unborn and has opened the doors of perception to an abundant variety of fetal behavior.

Using the advantages of 4D technology, it was possible to categorize embryonic and early fetal motor development for each week of gestation, beginning with seven weeks post menstruationem when the earliest embryonic movements appear. Understandably, the description and categorization of movements were repeatedly submitted to changes and amendments, as a result of improved resolution of fetal movements with new high-end 4D machines.

Seven weeks: Embryonic movements are rare. Bowing the head movements (gross body movement), no movements of limb buds.

8 to 9 weeks: The frequent embryonic movements can be divided into four groups (Fig. 35A):

1. Gross body movements (GM) consisting of complex movements of neck, trunk and limbs, involving the entire body, but without patterning or sequencing of any body parts, waxing and waning in intensity, force and speed, beginning and ceasing gradually. GMs emerge prior to isolated limb movements, and they can be observed before the completion of the spinal reflex arch which is accomplished at 8 weeks
2. Slow and small flexion, extension and sideways bending of the trunk, i.e. vermicular movements
3. Startles, representing a sudden fetal body movement lasting for about 1 second: Rapid phase contraction of all limb muscles
4. Limb movements with vigorous arm and leg movements.



Figs 35A (1 to 6): Fetal movements at 9 weeks with gross body, arm and leg movements



Figs 35B (1 to 10): 3D cine loop: Fetal general movements (GM) at 10+4 weeks survivor twin of dichorionic twin pregnancy with vanishing twin

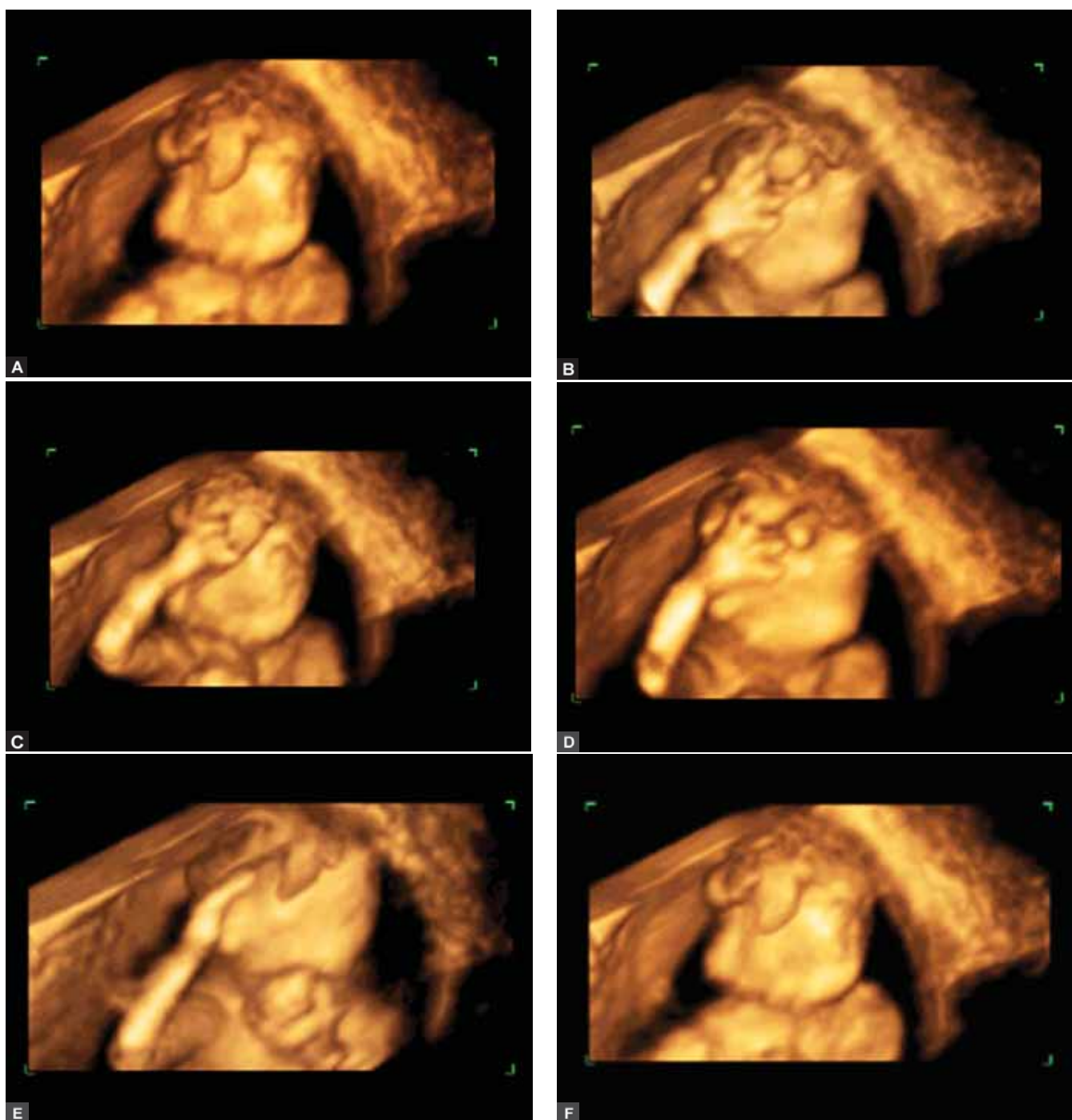
10 to 12 weeks: Elbow can be bended and stretched. Most common are now isolated arm movements. Complex body and limb movements already resemble movements of 3rd trimester fetuses and neonates: Twitching, floating, swimming, jumping, hick-ups, jaw movements, sucking, swallowing and yawning can be observed.⁸⁶

Any alteration of this movement pattern should be an indication for neurobehavioral follow-up examinations. Delay in motoric development with 1 to 2 weeks delay in the first appearance of all movement patterns has been described in diabetic pregnancies (Fig. 35B).⁸⁷

Neurobehavioral and limb development are obviously a dialectic process according to the concept of 'ontogenic adaptation', a terminus created by Prechtl et al.⁸⁸

Progressive degeneration of alpha motor neurons in the anterior horn of the spinal cord, and of motor nuclei in the brainstem, is the cause of arthrogryposis: Absence of limb movements results in joint contracture and spine deformation.⁸⁹

An interesting detail of early pregnancy 4D is the observation that early fetuses move their right arm more than their left one (lateralization). Clenched fist and so-called



Figs 36A to F: 4D: Vigorous arm movements of acranius at 15 weeks (Courtesy: Prof Asim Kurjak)



Figs 37A to C: 4D: 'Frozen' arm position and bilateral clenched fists with 'neurological thumb', acranium at 32 weeks gestation
(Courtesy: Prof Asim Kurjak)

'neurological thumb' as pathognomonic signs of trisomy 18 and/or syndromic diseases cannot be expected before 12 weeks gestation (Figs 36A to F) and (Figs 37A to C).⁹⁰

CONCLUSIONS

Ultrasound examination has become the 'gold standard' in assessment and follow-up of the development and of complications in early pregnancy. With introduction of transvaginal sonography, the accuracy of early morphological and biometrical ultrasound examinations has been significantly improved. The essential aim of an early pregnancy ultrasound is not only to diagnose a pregnancy, but also to differentiate between normal and abnormal pregnancy. The addition of color Doppler ultrasound has enabled functional hemodynamic evaluation soon after implantation. We speak of early pregnancy failure when a pregnancy ends spontaneously before the embryo has reached the gestational age in which visualization of a viable embryo should be possible.

The most common symptom of early pregnancy failure is vaginal bleeding. Transvaginal sonography is an ideal tool to examine patients who present with vaginal bleeding in the first and early second trimester, clarifying the differential diagnosis of missed abortion, ectopic pregnancy, blighted ovum and threatened abortion of a viable embryo. Viability can be established reliably by documenting cardiac activity in real-time, with B-mode and/or color Doppler ultrasonography. With a normal intrauterine pregnancy, bleeding from the chorion frondosum is undoubtedly the most common source of vaginal bleeding during the first trimester and should be considered as threatened abortion. Per definition, incomplete abortion is the passage of some, but not all, fetal or placental tissue through the cervical canal. In the case of a complete abortion, all products of conception are expelled through the cervix. Transvaginal ultrasonography including color Doppler plays the key role in assessing the uterine cavity after spontaneous abortion since it will detect retained products of conception. Retained products of conception after abortion may cause bleeding or endometritis. The diagnosis of missed abortion is determined by the ultrasound identification of an embryo/fetus without heart activity. It is relatively easy to make this diagnosis by means of transvaginal color Doppler ultrasound. The main parameter is

the absence of heartbeats in PW Doppler, and the lack of a color flow signals within the embryo after the 6th gestational week. Blighted ovum (anembryonic pregnancy) refers to a gestational sac in which the embryo either failed to develop or died at a stage too early for visualization. The diagnosis of anembryonic pregnancy is based on the absence of embryonic echoes within a gestational sac whose diameter/volume is large enough for such structures to be visualized, independent of the clinical data or menstrual cycle. Advances in transvaginal sonography permit early diagnosis of this abnormality at a mean sac diameter of 1.5 cm. To confirm the diagnosis, these findings should be correlated with other clinical and sonographic data including the presence of a yolk sac and serum beta hCG levels which are likely to show suboptimal ascent in an anembryonic pregnancy. Intrauterine hematomas are defined as sonolucent crescent or wedge-shaped areas between chorionic tissue and uterine wall, or fetal membranes. By localization, intrauterine hematomas can be divided into retroplacental, subchorionic, marginal and supracervical. The most severe are large, central, retroplacental hematomas. The prognosis for the pregnancy outcome is determined by two main elements: The location and the size of the hematoma. The essential color Doppler finding is that in the presence of hematomas, vascular resistance in the ipsilateral spiral arteries is increased and blood flow is decreased. Doppler measurements show lack of diastolic flow in most of hematomas, with RI of 1.0. The elevated impedance to blood flow is a transitory consequence of a compression of the spiral arterial walls by the hemorrhage itself.

The most common location of ectopic pregnancy is the fallopian tube. If at a serum beta hCG of 1500 mIU/ml (discriminatory zone) no intrauterine GS is visible with a high resolution TVS probe, then the situation is highly suspicious of ectopic pregnancy. The hypervascular 'rings of fire' of both ectopic pregnancy and corpus luteum graviditatis are often seen ipsilateral, with their characteristic low RI in pulsed Doppler.

Biometric and morphological characteristics of gestational sac and embryonic echo including the yolk sac can be used as predictive factors of abnormal early pregnancy. Decreased values of gestational sac diameter and/or its irregular shape can announce an upcoming incident and are used as markers for chromosomopathies. When GS growth-rate does not increase

at least by 0.7 mm per day, an early embryo failure should be considered.

The yolk sac is the first recognizable structure inside the gestational sac in early pregnancy. Primarily, the presence of an embryo without yolk sac before 10 weeks is an abnormal finding. Absence of the yolk sac, abnormal size of it, increased echogenicity, abnormal shape and abnormal number are predictive of early pregnancy failure. All these parameters should be assessed before 10 weeks of gestation.

Crown rump length (CRL) is used to define exact gestational age. The median CRL in fetuses with trisomies 21 and 13 or sex chromosome aneuploidies is not significantly different from that of a normal fetus. Mean amniotic sac diameter is approximately equal to the CRL in normal early pregnancy. Enlarged amniotic cavity in relation to CRL suggests early pregnancy abnormality.

First trimester screening: Increased nuchal translucency thickness at 11 to 13/6 weeks of gestation is associated with fetal chromosomal defects, many genetic syndromes and abnormalities, especially of the heart. Because of the change of the value of NT with CRL, each measurement of the NT should be compared with adequate CRL value. As additional independent markers for aneuploidy besides nuchal translucency have emerged the absence or hypoplasia of the nasal bone, tricuspid valve regurgitation and reverse A-wave of ductus venosus. They should be assessed too in case of increased NT.

Intracerebral translucency (IT) visible in the magnified midline-profile of the fetus, is a valuable extension of the 1st trimester screening to detect open neural tube defects. The caudal displacement of the hypoechoic structures of thalamus, cerebellum, pons and medulla oblongata causes early obliteration of the 4th ventricle, which changes the appearance of the IT accordingly.

Screening for pre-eclampsia at the time of 1st trimester screening: For a 5% false-positive rate, the combination of the following risk factors was shown to predict 90% of early onset pre-eclampsia, 35% of late onset pre-eclampsia and 20% of gestational hypertension: Maternal body mass index (BMI), age, ethnicity, smoking and parity, uterine artery pulsatility index (PI), maternal mean arterial pressure (MAP), maternal serum concentration of pregnancy-associated plasma protein-A (PAPP-A), maternal serum level of placental growth factor (PIGF). The Doppler assessment of the uterine artery pulsatility index is done via transabdominal or transvaginal approach.

Sonoembryology: Combined new ultrasound technologies, such as 3D, 4D, color, power and (with restrictions due to its potential thermogenic effect) pulsed wave Doppler have added many new sonographic details to the 'puzzle' of embryonic and early fetal period. A continuously growing evidence of normal findings in this stage of human development will certainly keep on modifying existing screening modules and enable earlier detection of abnormalities of the face, vertebra and spine, limbs, urinary system, chest (CCAM), abdominal wall and more.

Without much doubt there will be further technical improvement of ultrasonographic tools allowing us new and deeper insights into *in vivo* conditions of the beginnings of human life.

REFERENCES

- Zafar NB, Greer V, Woolard RH. The use of transvaginal ultrasound by emergency physicians in medical student education. *Donald School Journal of Ultrasound in Obstetrics and Gynecology* 2009;3(4):59-64.
- Kurjak A, Kupesic S, Carrera JM, Ahmed B. Ultrasound evaluation of abnormal early pregnancy. *Donald School Journal of Ultrasound in Obstetrics and Gynecology* 2008;2(2):87-105.
- Kurjak A, Schulman H, Kupesic S, Zudenigo D, Kos M, Goldenberg M. Subchorionic hematomas in early pregnancy: Clinical outcome and blood flow patterns. *J Matern Fetal Med* 1996;5:41-44.
- 1990-1992 MMWR Morb Mortal Wkly Rep 1995;44:46.
- Fylstra DL. Tubal Pregnancy: A review of current diagnosis and treatment. *Obstet Gynecol Surv* 1998;53:320.
- Murray H, Baakdak H, Tulandi H, Bardell T. Diagnosis and treatment of ectopic pregnancy. *CM AJ* 2005;173:905.
- Yao M, Tulandi T. Current status of surgical treatment of ectopic pregnancy. *Fertil Steril* 1997;67:421.
- Kurjak A, Zalud I, Shulman H. Ectopic pregnancy: Transvaginal color Doppler of trophoblastic flow in questionable adnexa. *J Ultrasound Med* 1991;10:685-89.
- Kupesic S. Ectopic pregnancy. In: *Ian Donald School Textbook of Ultrasound in Obstetrics and Gynecology* (2nd ed). Jaypee Brothers: New Delhi 2008;230-43.
- Honemeyer U. Primary care in obstetrics and gynecology: A place for advanced ultrasound. *Donald School Journal of Ultrasound in Obstetrics and Gynecology* 2009;3(3):61-74.
- McAuliffe FM, Fong KW, Toi A, Chitayat D, Keating S, Johnson JA. Ultrasound detection of fetal anomalies in conjunction with 1st trimester nuchal translucency screening: A feasibility study. *American Journal of Obstetrics and Gynecology* 2005;193:1260-65.
- Souka, et al. Assessment of fetal anatomy at the 11 to 14 weeks ultrasound examination. *Ultrasound Obstet Gynecol* 2004;24:730-34.
- ACOG practice patterns. Routine ultrasound in low-risk pregnancies. *Int Journal of Gynecol Obstet* 1997;59:273-78.
- Laurel MD. American Institute of Ultrasound in Medicine. Guidelines for the performance of the antepartum obstetrical examination 1994.
- Crane JP, LeFevre ML, Winborn RC, et al. RADIUS study group. A randomized trial of prenatal ultrasound screening: Impact on the detection, management, and outcome of anomalous fetus. *Am J Obstet Gynecol* 1994;171:392-99.
- Theodora M, Daskalakis G, Antsaklis A. Screening for fetal malformations. *Donald School Journal of Ultrasound in Obstetrics and Gynecology* 2008;2(1):6-15.
- Maeda K. Safety of ultrasound in fetal diagnosis. *Donald School Journal of Ultrasound in Obstetrics and Gynecology* 2008;2(2):12-16.
- Chervenak FA, McCullough LB. The ethics of implementing first trimester risk assessment. *Donald School Journal of Ultrasound in Obstetrics and Gynecology* 2008;2(2):57-61.
- Kagan KO, Wright D, Valencia C, et al. Screening for trisomies 21,18,13 by maternal age, fetal nuchal translucency, fetal heart rate, free beta hCG, and pregnancy-associated plasma protein-A. *Human Reprod Sep* 23:1968-57, Epub 2008 June 10.

20. Antsaklis A, Partsinevelos GA. First trimester screening for chromosomal abnormalities. *Donald School Journal of Ultrasound in Obstetrics and Gynecology* 2008;2(1):20-28.
21. Vis JC, Duffels MGJ, Winter, et al. Down syndrome: A cardiovascular perspective. *J Intellect Disabil Res* 2009;53:419-25 (Epub Feb 18 2009).
22. Chaoui R, Benoit B, Mitkowska-Wozniak K, et al. Assessment of intracranial translucency (IT) in the detection of spina bifida at the 11-13 weeks scan. *Ultrasound Obstet Gynecol* 2009;34:249-52.
23. Page EW. The relation between hydatid moles, relative ischemia of the gravid uterus, and the placental origin of preeclampsia. *Am J Obstet Gynecol* 1939;37:291-93.
24. Rosenberg KR, Trevathin WR. An anthropological perspective on the evolutionary context of pre-eclampsia in humans. *J Reprod Immunol* 2007;76(1-2):91-97.
25. Robillard PY, Hulsey TC, Dekker GA, Chaouat G. Pre-eclampsia and human reproduction. An essay of a long-term reflection. *J Reprod Immunol* 2003;59(2):93-100.
26. Roberts JM, Gammil HS. Pre-eclampsia recent insights. *Hypertension* 2005;46:12-43.
27. Roberts JM, Redman CW. Pre-eclampsia: More than pregnancy-induced hypertension. *Lancet* 1993;341:1447.
28. Meekins JW, Pijnenborg R, Hanssens M, et al. A study of placental bed spiral arteries and trophoblast invasion in normal and severe pre-eclamptic pregnancies. *Br J Obstet Gynecol* 1994;101:669.
29. Jauniaux E, Watson AL, Hempstockj, Bao YP, Skepper JN, Burton GJ. Onset of maternal arterial blood flow and placental oxidative stress: A possible factor in human early pregnancy failure. *Am J Pathol* 2000;157:2111-22.
30. King A, Hiby S, Gardner L, Joseph S, Bowen J, Verma S, et al. Recognition of trophoblast HLA class 1 molecules by decidual NK cell receptors: A review. *Placenta* 2000;21(suppl A):81-85.
31. Allaire AD, Ballenger KA, Wells SR, McMahon MJ, Lessey BA. Placental apoptosis in pre-eclampsia. *Obstet Gynecol* 2000;96:271-76.
32. Knight M, Redman CW, Linton EA, Sargent IL. Shedding of syncytiotrophoblast microvilli into maternal circulation in pre-eclamptic pregnancies. *Br J Obstet Gynecol* 1998;105:632-40.
33. Cowans NJ, Stamatoopoulou A, Matwejew E, von Kaisenberg CS, Spencer K. First trimester placental growth factor as a marker for hypertensive disorders and SGA. *Prenat Diagn* 2010;30(6):565-70.
34. Chaiworapongsa T, Romero R, Espinoza J, et al. Evidence for supporting a role of blockade of the vasculat endothelial growth factor system in the pathophysiology of preeclampsia. Young investigator award. *Am J Obstet Gynecol* 2004;190:1541.
35. Romero R, Nien JK, Espinoza J, et al. A longitudinal study of angiogenic (PGF) and antiangiogenic (sEng and sFLT) factors in normal pregnancy and patients destined to develop pre-eclampsia and deliver SGA neonates. *J Matern Fetal Neonatal Med* 2008;21(1):9-23.
36. Romero R, Chaiwarapongsa T, Erez O, et al. An imbalance between angiogenic and antiangiogenic factors precedes fetal death in a subset of patients: Results of a longitudinal study. *J Matern Fetal Neonatal Med* 2010 May (Epub ahead of print).
37. Masuyama H, Segawa T, Sumida Y, et al. Different profiles of circulating angiogenic factors and adipocytokines between early and late onset preeclampsia. *BJOG* 2010;117(3):314-20.
38. Poon LCY, Staboulidou I, Maiz N, et al. Hypertensive disorders in pregnancy: Screening by uterine artery Doppler at 11-13 weeks. *Ultrasound Obstet Gynecol* 2009;34:142-48.
39. Sonek JD. First trimester ultrasound screening: An update. *Donald School Journal of Ultrasound in Obstetrics and Gynecology* 2010;4(2):97-116.
40. Bonilla-Musoles F, Raga F, Bonilla F, Jr, Machado LE, Osborne NG, Ruiz F, Castillo JC. Prune Belly syndrome versus posterior urethral valve. Ahead of Publication.
41. Pooh RK, Kurjak A. Recent advances in 3D assessment of various fetal anomalies. *Donald School Journal of Ultrasound in Obstetrics and Gynecology* 2009;3(3):1-23.
42. Leung KY, Cheong KB, Tang MHY. 2D and 3D ultrasound prediction of homozygous alpha 0-thalassemia. *Donald School Journal of Ultrasound in Obstetrics and Gynecology* 2010;4(2):123-26.
43. Lausin I, Kurjak A, Pooh RK, Azumendi G, Maeda K. Advances in visualisation of the early human development. *Donald School Journal of Ultrasound in Obstetrics and Gynecology* 2009;3(3):25-38.
44. Blaas HG, Eik-Nes SH, Isaksen CV. The detection of spina bifida before 10 gestational weeks using two- and three-dimensional ultrasound. *Ultrasound Obstet Gynecol* 2000;16:20-29.
45. Marton I, Kurjak A, Azumendi G, Al-Noobi M, Perva S. Study of fetal neurodevelopment in multiple pregnancies. *Donald School Journal of Ultrasound in Obstetrics and Gynecology* 2009;3(3):51-60.
46. Arabin B, Bos R, Rijlardsdam R, et al. The onset of inter-human contacts. Longitudinal ultrasound observations in twin pregnancies. *Ultrasound Obstet Gynecol* 1996;8:166-73.
47. Talic A, Honemeyer U. Cerebral palsy: State of art. *Donald School Journal of Ultrasound in Obstetrics and Gynecology* 2010;4(2):189-98.
48. McLorie G, Baskin LS, Kim MS. Management of vesicourethral reflux. UpToDate October 2010.
49. Azumendi G, Kurjak A. Three-dimensional sonoembryology. *Donald School Journal of Ultrasound in Obstetrics and Gynecology* 2008;2(2):62-86.
50. Sadler TW. *Langman's Medical Embryology*. (9th ed). Lippincott Williams & Wilkins. (Part 2) Ch. 5 2004;102.
51. Green JJ, Hobbins JC. Abdominal ultrasound examination of the first trimester fetus. *Am J Obstet Gynecol* 1988.
52. Kupesic S, Kurjak A. Volume and vascularity of yolk sac assessed by three-dimensional and power Doppler ultrasound. *Early Pregnancy* 2001;5(1):40-41.
53. Kurjak A, Kupesic S. Parallel Doppler assessment of yolk sac and intervillous circulation in normal pregnancy and missed abortion. *Placenta* 1998;19:619-23.
54. Ikonomou T, Theodora M. Prenatal screening for congenital heart defects. *Donald School Journal of Ultrasound in Obstetrics and Gynecology* 2008;2(1):16-19.
55. Allan LD, Sharland GK, Chita SK, Lockhart S, Maxwell DJ. Chromosomal anomalies in fetal heart congenital disease. *Ultrasound Obstet Gynecol* 1991;1:8-11.
56. Pilu G, Nicolaidis KH. *Diagnosis of fetal abnormalities: The 18 to 23 weeks scan*. Parthenon Publishing 1999.
57. Buskens E, Grobbee DE, Frohn-Mulder IM, et al. Efficacy of routine fetal ultrasound screening for congenital heart disease in normal pregnancy. *Circulation* 1996;1:67-72.
58. Achiron R, Weissman A, Rotstein Z, Lipitz S, Mashiach S, Hegesh J. Transvaginal echocardiographic examination of the fetal heart between 13 and 15 weeks of gestation in a low-risk population. *J Ultrasound Med* 1994;13:783-89.
59. Turan S, Turan OM, Torredes TY, Harman CR, Baschat AA. Standardization of the first-trimester fetal cardiac examination using spatiotemporal image correlation with tomographic ultrasound and color Doppler imaging. *Ultrasound Obstet Gynecol* 2009;33:652-56.

60. Predanic M. Sonographic assessment of the umbilical cord. *Donald School Journal of Ultrasound in Obstetrics and Gynecology* 2009;3(2):48-57.
61. Berg C, Kremer C, Geipel A, Kochl T, Germer U, Gembruch U. Ductus venosus blood flow alterations in fetus with obstructive lesion of the right heart. *Ultrasound Obstet Gynecol* 2006;28:137-42.
62. Nicolaides KH, Wegrzyn P. Increased nuchal translucency with normal karyotype. *Ginecol Pol* Aug 2005;76(8):593-601.
63. Orosz L, Lukacs J, Szabo M, Kovacs T, Zsupan I, Orosz G, et al. Long-term outcome of pregnancies with increased nuchal translucency and normal karyotype. *Donald School Journal of Ultrasound in Obstetrics and Gynecology* 2009;3(3):83-89.
64. Wiechec M, Nocun A, Beithon J. Early fetal echocardiography at the time of 11+0 to 13+6 weeks scan. *Donald School Journal of Ultrasound in Obstetrics and Gynecology* 2009;3(3):75-81.
65. Carvalho JS. Fetal heart scanning in the first trimester. *Prenat Diagn* 2004;24:1060-67.
66. Harmath A, Hajdu J, Hauzman E, Pete B, Papp Z. Surgical and dysmorphological aspects of abdominal wall defects. *Donald School Journal of Ultrasound in Obstetrics and Gynecology* 2009;3(2):38-47.
67. Arnaoutoglou C, Pasqiuni L, Abel R, Kumar S. Outcome of antenatally diagnosed fetal anterior abdominal wall defects from a single tertiary center. *Fetal Diagn Ther* 2008;24:416-19.
68. David AL, Tan A, Curry J. Gastroschisis: Sonographic diagnosis, associations, management, and outcome. *Prenat Diagn* 2008;28:633-44.
69. Harmath A, Hajdu J, Hauzman E, Pete B, Papp Z. Surgical and dysmorphological aspects of abdominal wall defects. *Donald School Journal of Ultrasound in Obstetrics and Gynecology* 2009;3(2):38-47.
70. Mann S, Blinmann TA, Wilson RD. Prenatal and postnatal management of omphalocele. *Prenat Diagn* 2008;28:626-32.
71. Smrcek JM, Germer U, Krokowski M, Berg C, Krapp M, et al. Prenatal ultrasound diagnosis and management of body stalk anomaly: Analysis of nine singleton and two multiple pregnancies. *Ultrasound Obstet Gynecol* 2003;21:322-28.
72. Peixoto-Filho FM, Cima LC, Nakamura, Pereira M. Prenatal diagnosis of pentalogy of Cantrell in the 1st trimester: Is three-dimensional ultrasound needed? *J Clin Ultrasound* 2008;37:112-14.
73. Tiblad E, Wilson RD, Carr M, Flake AW, Hedrick H, et al. OEIS sequence: A rare congenital anomaly with prenatal evaluation and postnatal outcome in six cases. *Prenat Diagn* 2008;28:141-47.
74. Azumendi G, Lausin I, Kurjak A, Pooh RK, Grant G. Ultrasonographic evaluation of fetal face by 3D/4D sonography. *Donald School Journal of Ultrasound in Obstetrics and Gynecology* 2008;2(4):45-57.
75. Evans DJ, Francis-West PH. Craniofacial development making faces. *J Anat* 2005;207:435-36.
76. Kurjak A, Pooh RK, Merce LT, Carrera JM, Salihagic-Kadic A, Andonotopo W. Structural and functional early human development assessed by three-dimensional (3D) and four-dimensional (4D) sonography. *Fertil Steril* 2005;84(5):1285-99.
77. Kostovic I, Judas M. Maturation of cerebral connections and fetal behaviour. *Donald School Journal of Ultrasound in Obstetrics and Gynecology* 2008;2(3):80-86.
78. Yakovlev PI, Lecours AR. The myelogenetic cycles of regional maturation of the brain. In: A Minkowski (Ed): *Regional development of the brain in early life*. Blackwell, Oxford 1967;3-70.
79. Shiota K. Embryology of the human brain. *Donald School Journal of Ultrasound in Obstetrics and Gynecology* 2008;2(3):1-8.
80. Pooh RK, Kurjak A. Neuroscan of normal and abnormal vertebrae and spinal cord. *Donald School Journal of Ultrasound in Obstetrics and Gynecology* 2008;2(3):9-18.
81. Gray DL, Crane JP, Rudloff MA. Prenatal diagnosis of neural tube defects: Origin of midtrimester vertebral ossification centers as determined by sonographic water-bath studies. *J Ultrasound Med* 1988;7:421-27.
82. Prechtl HFR. Qualitative changes of spontaneous movements in fetus and preterm infant are a marker of neurological dysfunction. *Early Hum Dev* 1990;23:151-58.
83. Salihagic-Kadic A, Predojevic M, Kurjak A. Advances in fetal neurophysiology. In: *Fetal Neurology*. Pooh RK, Kurjak A, Jaypee Brothers: New Delhi 2009;161-219.
84. Stafstrom CE, et al. Spontaneous neural activity in fetal brain reaggregate culture. *Neuroscience* 1980;1681-89.
85. Joseph R. Fetal brain and cognitive development. *Dev Rev* 1999;20:81-98.
86. Kurjak A, Ahmed B, Miskovic B, Predojevic M, Salihagic Kadic A. Fetal behaviour assessed by 4D sonography. In: Kurjak A, Chervenak FA. *Donald School Textbook of Ultrasound in Obstetrics and Gynecology*. Jaypee Brothers: New Delhi 2011.
87. Mulder EJ, Visser GH. Growth and motor development in fetuses of mothers with type-1 diabetes. Emergence of specific movement patterns. *Early Hum Dev* 1991;25:107.
88. Kurjak A, Pooh RK, Tikvica A, Stanojevic M, Miskovic B, Ahmed B, Azumendi G. Assessment of fetal neurobehavior by 3D-4D ultrasound. In: Pooh RK, Kurjak A. *Fetal neurology*. Jaypee Brothers: New Delhi 2009:222-85.
89. Kurjak A, Veccek N, Hafner T, Bozek T, Kurjak BF, Ujevic B. Prenatal diagnosis: What does four-dimensional ultrasound add? *J Perinat Med* 2002;30:57-62.
90. Pooh RK, Kurjak A. Normal and abnormal fetal hands/fingers positioning and movement in the first and early second trimester detected by 3D/4D ultrasound. In: Pooh RK, Kurjak A. *Fetal Neurology*. Jaypee Brothers: New Delhi 2009:315-28.